

# Bootstrap prediction bands for functional time series

Efstathios Paparoditis

Department of Mathematics and Statistics

University of Cyprus

and

Han Lin Shang

Department of Actuarial Studies and Business Analytics

Macquarie University

## Abstract

A bootstrap procedure for constructing prediction bands for a stationary functional time series is proposed. The procedure exploits a general vector autoregressive representation of the time-reversed series of Fourier coefficients appearing in the Karhunen-Loève representation of the functional process. It generates backward-in-time functional replicates that adequately mimic the dependence structure of the underlying process in a model-free way and have the same conditionally fixed curves at the end of each functional pseudo-time series. The bootstrap prediction error distribution is then calculated as the difference between the model-free, bootstrap-generated future functional observations and the functional forecasts obtained from the model used for prediction. This allows the estimated prediction error distribution to account for the innovation and estimation errors associated with prediction and the possible errors due to model misspecification. We establish the asymptotic validity of the bootstrap procedure in estimating the conditional prediction error distribution of interest, and we also show that the procedure enables the construction of prediction bands that achieve (asymptotically) the desired coverage. Prediction bands based on a consistent estimation of the conditional distribution of the studentized prediction error process also are introduced. Such bands allow for taking more appropriately into account the local uncertainty of the prediction. Through a simulation study and the analysis of two data sets, we demonstrate the capabilities and the good finite-sample performance of the proposed method.

*Keywords:* Functional prediction; Prediction error; Principal components; Karhunen-Loève expansion.

# 1 Introduction

Functional time series consist of random functions observed at regular time intervals. They can be classified into two main categories depending on whether the continuum is also a time variable. First, functional time series can arise from measurements obtained by separating an almost continuous time record into consecutive intervals (e.g., days, weeks, or years; see, e.g., [Hörmann & Kokoszka 2012](#)). We refer to such data structures as sliced functional time series, examples of which include daily price curves of a financial stock ([Kokoszka et al. 2017](#)) and intraday particulate matter ([Shang 2017](#)). When the continuum is not a time variable, functional time series can also arise when observations over a period are considered as finite-dimensional realizations of an underlying continuous function (e.g., yearly age-specific mortality rates; see, e.g., [Chiou & Müller 2009](#), [Hyndman & Shang 2009](#)).

In either case, the underlying strictly stationary stochastic process is denoted by  $\mathbf{X} = \{\mathcal{X}_t, t \in \mathbb{Z}\}$ , where each  $\mathcal{X}_t$  is a random element in a separable Hilbert space  $\mathcal{H}$ , with values  $\mathcal{X}_t(\tau)$  and  $\tau$  varying within a compact interval  $\mathcal{I} \subset \mathbb{R}$ . We assume that  $\mathcal{I} = [0, 1]$  without loss of generality. Furthermore, we assume that  $\mathcal{H} = L^2$ , the set of (equivalence classes of) measurable, real-valued functions  $x(\cdot)$  defined on  $[0, 1]$  and satisfying  $\int_0^1 x^2(\tau) d\tau < \infty$ . Central statistical issues include modeling of the temporal dependence of the functional random variables  $\{\mathcal{X}_t, t \in \mathbb{Z}\}$ , making inferences about parameters of interest, and predicting future values of the process when an observed stretch  $\mathcal{X}_1, \mathcal{X}_2, \dots, \mathcal{X}_n$  is given. Not only is it vital to obtain consistent estimators, but to also estimate the uncertainty associated with such estimators, the construction of confidence or prediction intervals, and the implementation of hypothesis tests (e.g., [Horváth et al. 2014](#)). When such inference problems arise in functional time series, a resampling methodology, especially bootstrapping, is an important alternative to standard asymptotic considerations. For independent and identically distributed (i.i.d.) functional data, bootstrap procedures have been considered, among others, by [Cuevas et al. \(2006\)](#), [McMurry & Politis \(2011\)](#), [Goldsmith et al. \(2013\)](#), [Shang \(2015\)](#), [Paparoditis & Sapatinas \(2016\)](#), where appropriate sampling from the observed sample is used to mimic sampling from the population. However, for functional time series, the existing temporal dependence between the random elements  $\mathcal{X}_t$  significantly complicates matters, and the bootstrap must be appropriately adapted in order to be successful.

The development of bootstrap procedures for functional time series has received increasing attention in recent decades. In an early paper, [Politis & Romano \(1994\)](#) obtained weak convergence results for approximate sums of weakly dependent, Hilbert space-valued random variables. [Dehling](#)

et al. (2015) also obtained weak convergence results for Hilbert space valued random variables, which are assumed to be weakly dependent in the sense of near-epoch dependence and showed consistency of a non-overlapping block bootstrap procedure. Raña et al. (2015) extended the stationary bootstrap to functional time series, Ferraty & Vieu (2011) applied a residual-based bootstrap procedure to construct confidence intervals for the regression function in a nonparametric setting, and Zhu & Politis (2017) to kernel estimators. Franke & Nyarige (2019) proposed a residual-based bootstrap procedure for functional autoregressions. Pilavakis et al. (2019) established theoretical results for the moving block and the tapered block bootstrap, Shang (2018) applied a maximum entropy bootstrap procedure, and Paparoditis (2018) proposed a sieve bootstrap for functional time series.

In this paper, we build on the developments mentioned above and focus on constructing prediction intervals or bands for a functional time series. To elaborate, suppose that for every  $t \in \mathbb{Z}$ , the zero mean random element  $\mathcal{X}_t$  is generated as

$$\mathcal{X}_t = f(\mathcal{X}_{t-1}, \mathcal{X}_{t-2}, \dots) + \varepsilon_t, \quad (1)$$

where  $f : \mathcal{H}^\infty \rightarrow \mathcal{H}$  is some appropriate operator and  $\{\varepsilon_t\}$  is a zero mean i.i.d. innovation process in  $\mathcal{H}$  with  $E\|\varepsilon_t\|^2 < \infty$  and  $\|\cdot\|$  the norm of  $\mathcal{H}$ . For simplicity, we write  $\varepsilon_t \sim i.i.d.(0, C_\varepsilon)$ , where  $C_\varepsilon = E(\varepsilon_t \otimes \varepsilon_t)$  is the covariance operator of  $\varepsilon_t$  and  $\otimes$  denotes the tensor operator, defined by  $(x \otimes y)(\cdot) = \langle x, \cdot \rangle y$ , for  $x, y \in \mathcal{H}$ . Suppose that based on the last  $k$  observed functional elements,  $\mathcal{X}_n, \mathcal{X}_{n-1}, \dots, \mathcal{X}_{n-k+1}$ ,  $k < n$ , a predictor

$$\hat{\mathcal{X}}_{n+h} = \hat{g}_{(h)}(\mathcal{X}_n, \mathcal{X}_{n-1}, \dots, \mathcal{X}_{n-k+1}), \quad (2)$$

of  $\mathcal{X}_{n+h}$  is used, where  $h \in \mathbb{N}$  is the prediction horizon and  $\hat{g}_{(h)} : \mathcal{H}^k \rightarrow \mathcal{H}$  some estimated operator. For instance, we may think of  $\hat{g}_{(h)}$  as an estimator of the best predictor, i.e., of the conditional expectation  $E(\mathcal{X}_{n+h} | \mathcal{X}_n, \mathcal{X}_{n-1}, \dots, \mathcal{X}_{n-k+1})$ . The important case, however, we have in mind, is that where a model

$$\mathcal{X}_t = g(\mathcal{X}_{t-1}, \mathcal{X}_{t-2}, \dots, \mathcal{X}_{t-k}) + v_t, \quad (3)$$

is used to predict  $\mathcal{X}_{n+h}$ . Here  $g : \mathcal{H}^k \rightarrow \mathcal{H}$  is an unknown, linear bounded operator and  $v_t \sim i.i.d.(0, C_v)$ . Using model (3), a  $h$ -step-ahead predictor can be obtained as

$$\hat{\mathcal{X}}_{n+h} = \hat{g}(\hat{\mathcal{X}}_{n+h-1}, \hat{\mathcal{X}}_{n+h-2}, \dots, \hat{\mathcal{X}}_{n+h-k}), \quad (4)$$

where  $\hat{g}$  is an estimator of the operator  $g$  in (3) and  $\hat{\mathcal{X}}_t \equiv \mathcal{X}_t$ , if  $t \in \{n-k+1, n-k+2, \dots, n\}$ . Notice that the predictor (4) also can be written as  $\hat{\mathcal{X}}_{n+h} = \hat{g}_{(h)}(\mathcal{X}_n, \mathcal{X}_{n-1}, \dots, \mathcal{X}_{n-k+1})$

for some appropriate operator  $\widehat{g}_{(h)}$ . In particular, setting  $\widehat{g}_{(1)} = \widehat{g}$ , it is easily seen that  $\widehat{g}_{(h)} = \widehat{g}(\widehat{g}_{(h-1)}, \dots, \widehat{g}_{(1)}, \mathcal{X}_n, \dots, \mathcal{X}_{n-k+h})$  for  $2 \leq h \leq k$  and  $\widehat{g}_{(h)} = \widehat{g}(\widehat{g}_{(h-1)}, \dots, \widehat{g}_{(h-k)})$  for  $h > k$ . We stress here the fact that we do not assume that model (3) used for prediction coincides with the true data generating process (1); that is, we allow for model misspecification. Observe that the simple case, where  $g$  is known up to a finite-dimensional vector of parameters, is also covered by the above setup.

As already mentioned, our aim is to construct a prediction band for  $\mathcal{X}_{n+h}$  associated with the predictor  $\widehat{\mathcal{X}}_{n+h}$ . That is, given the part  $\mathcal{X}_{n,k} = (\mathcal{X}_n, \mathcal{X}_{n-1}, \dots, \mathcal{X}_{n-k+1})$  of the functional time series observed and for any  $\alpha \in (0, 1)$ , we want to construct a band denoted by  $\{[\widehat{\mathcal{X}}_{n+h}(\tau) - L_{n,h}(\tau), \widehat{\mathcal{X}}_{n+h}(\tau) + U_{n,h}(\tau)], \tau \in [0, 1]\}$  such that

$$\lim_{n \rightarrow \infty} P\left(\widehat{\mathcal{X}}_{n+h}(\tau) - L_{n,h}(\tau) \leq \mathcal{X}_{n+h}(\tau) \leq \widehat{\mathcal{X}}_{n+h}(\tau) + U_{n,h}(\tau), \text{ for all } \tau \in [0, 1] \middle| \mathcal{X}_{n,k}\right) = 1 - \alpha.$$

Toward this end we focus on the estimation of the conditional distribution of the prediction error  $\mathcal{E}_{n+h} = \mathcal{X}_{n+h} - \widehat{\mathcal{X}}_{n+h}$  given  $\mathcal{X}_{n,k}$ , which is a key quantity for the construction of the prediction band of interest. Using (4), this error can be decomposed as

$$\begin{aligned} \mathcal{E}_{n+h} &:= \mathcal{X}_{n+h} - \widehat{\mathcal{X}}_{n+h} \\ &= \varepsilon_{n+h} \\ &\quad + \left[ f(\mathcal{X}_{n+h-1}, \mathcal{X}_{n+h-2}, \dots) - g(\mathcal{X}_{n+h-1}, \mathcal{X}_{n+h-2}, \dots, \mathcal{X}_{n+h-k}) \right] \\ &\quad + \left[ g(\mathcal{X}_{n+h-1}, \mathcal{X}_{n+h-2}, \dots, \mathcal{X}_{n+h-k}) - \widehat{g}(\widehat{\mathcal{X}}_{n+h-1}, \widehat{\mathcal{X}}_{n+h-2}, \dots, \widehat{\mathcal{X}}_{n+h-k}) \right] \\ &= \mathcal{E}_{I,n+h} + \mathcal{E}_{M,n+h} + \mathcal{E}_{E,n+h}, \end{aligned}$$

with an obvious notation for  $\mathcal{E}_{I,n+h}$ ,  $\mathcal{E}_{M,n+h}$  and  $\mathcal{E}_{E,n+h}$ . Notice that  $\mathcal{E}_{I,n+h}$  is the error attributable to the i.i.d. innovation,  $\mathcal{E}_{M,n+h}$  is the model specification error, and  $\mathcal{E}_{E,n+h}$  is the error attributable to estimation of the unknown operator  $g$  and of the random elements  $\mathcal{X}_{n+h-1}, \dots, \mathcal{X}_{n+h-k}$  used for  $h$ -step prediction. Observe that if  $h = 1$  then  $\mathcal{E}_{E,n+1}$  only depends on the estimation error  $\widehat{g} - g$ . Furthermore, if  $\widehat{g}$  is a consistent estimator of  $g$ , for instance, if  $\|\widehat{g} - g\|_{\mathcal{L}} \xrightarrow{P} 0$ , with  $\|\cdot\|_{\mathcal{L}}$  being the operator norm, the part of the estimation error  $\mathcal{E}_{E,n+h}$  which is due to the estimator  $\widehat{g}$  is asymptotically negligible. On the contrary, the misspecification error  $\mathcal{E}_{M,n+h}$  may not vanish asymptotically if the model used for prediction is different from the one generating the data.

To better illustrate the above discussion, consider the following example. Suppose that  $\mathcal{X}_t$  is generated according to the FAR(2) model  $\mathcal{X}_t = \Phi_1(\mathcal{X}_{t-1}) + \Phi_2(\mathcal{X}_{t-2}) + \varepsilon_t$ ,  $\Phi_2 \neq 0$ , and that a FAR(1) model  $\mathcal{X}_t = R(\mathcal{X}_{t-1}) + v_t$  is used for prediction, where  $\Phi_1$ ,  $\Phi_2$ , and  $R$  are appropriate

operators. In general,  $R \neq \Phi_1$ . With  $\widehat{R}$  denoting an estimator of  $R$ , the prediction error  $\mathcal{E}_{n+h}$  can be decomposed as

$$\mathcal{X}_{n+h} - \widehat{\mathcal{X}}_{n+h} = \varepsilon_{n+h} + (\Phi_1(\mathcal{X}_{n+h-1}) - R(\mathcal{X}_{n+h-1}) + \Phi_2(\mathcal{X}_{n+h-2})) + (R(\mathcal{X}_{n+h-1}) - \widehat{R}(\widehat{\mathcal{X}}_{n+h-1})).$$

Consider now the conditional distribution  $\mathcal{E}_{n+h}|\mathcal{X}_n$ . Notice that if  $h = 1$ , the model specification error  $(\Phi_1(\mathcal{X}_n) - R(\mathcal{X}_n) + \Phi_2(\mathcal{X}_{n-1}))$  causes a shift in this conditional distribution due to the term  $\Phi_1(\mathcal{X}_n) - R(\mathcal{X}_n)$  as well as an increase in variability due to the term  $\Phi_2(\mathcal{X}_{n-1})$ . Similarly, for  $h \geq 2$  the model specification error  $(\Phi_1(\mathcal{X}_{n+h-1}) - R(\mathcal{X}_{n+h-1}) + \Phi_2(\mathcal{X}_{n+h-2}))$  does not vanish asymptotically. Furthermore, for  $h \geq 2$ , the error  $(R(\mathcal{X}_{n+h-1}) - \widehat{R}(\widehat{\mathcal{X}}_{n+h-1}))$  is not only due to the estimator  $\widehat{R}$  of  $R$  (as in the case  $h = 1$ ), but also due the fact that the unknown random element  $\mathcal{X}_{n+h-1}$  has been replaced by its predictor  $\widehat{\mathcal{X}}_{n+h-1}$ . This causes a further increase in variability.

An appropriate procedure to construct prediction intervals or bands, should consider *all three* aforementioned sources affecting the prediction error and consistently estimate the conditional distribution  $\mathcal{E}_{n+h}|\mathcal{X}_n, \mathcal{X}_{n-1}, \dots, \mathcal{X}_{n-k+1}$ . However, and to the best of our knowledge, this issue has not been appropriately explored in the literature. In particular, and even in the most studied univariate, real-valued case, it is common to estimate the prediction error distribution by ignoring the model specification error, that is, by assuming that the model used for prediction is identical to the data generating process. Consequently, the bootstrap approaches applied in this context, use the same model to make the prediction and to generate the bootstrap pseudo-time series. Such approaches ignore the model misspecification error; see [Thombs & Schucany \(1990\)](#), [Breidt et al. \(1995\)](#), [Alonso et al. \(2002\)](#), [Pascual et al. \(2004\)](#) as well as [Pan & Politis \(2016\)](#) and the references therein. See also Section 3 for more details.

In this paper, we develop a bootstrap procedure to construct prediction bands for functional time series that appropriately takes into account *all three* sources of errors affecting the conditional distribution of  $\mathcal{E}_{n+h}$ . The proposed bootstrap approach generates, in a model-free way, pseudo-replicates  $\mathcal{X}_1^*, \mathcal{X}_2^*, \dots, \mathcal{X}_n^*$ , and  $\mathcal{X}_{n+1}^*, \mathcal{X}_{n+2}^*, \dots, \mathcal{X}_{n+h}^*$  of the functional time series at hand that appropriately mimic the dependence structure of the underlying functional process. Moreover, the approach ensures that the generated functional pseudo-time series has the same  $k$  functions at the end as the functional times series observed; that is,  $\mathcal{X}_t^* = \mathcal{X}_t$  holds true for  $t \in \{n - k + 1, n - k + 2, \dots, n\}$ . This is important because, as already mentioned, it is the conditional distribution of  $\mathcal{E}_{n+h}$  given  $\mathcal{X}_n, \mathcal{X}_{n-1}, \dots, \mathcal{X}_{n-k+1}$  in which we are interested. These requirements are fulfilled by generating the functional pseudo-elements  $\mathcal{X}_1^*, \mathcal{X}_2^*, \dots, \mathcal{X}_n^*$  using a backward-in-time vector autoregressive representation of the time-reversed process of scores appearing in the Karhunen-

Loève representation (see Section 2 for details). Given the model-free, bootstrap-generated functional pseudo-time series  $\mathcal{X}_1^*, \mathcal{X}_2^*, \dots, \mathcal{X}_n^*$  and  $\mathcal{X}_{n+1}^*, \dots, \mathcal{X}_{n+h}^*$ , the same model used to obtain the predictor  $\hat{\mathcal{X}}_{n+h} = \hat{g}(\hat{\mathcal{X}}_{n+h-1}, \dots, \hat{\mathcal{X}}_{n+h-k})$ , see (4), is then applied, and the pseudo-predictor  $\hat{\mathcal{X}}_{n+h}^* = \hat{g}^*(\hat{\mathcal{X}}_{n+h-1}^*, \dots, \hat{\mathcal{X}}_{n+h-k}^*)$  is obtained. Here,  $\hat{\mathcal{X}}_t^* = \mathcal{X}_t^* = \mathcal{X}_t$  if  $t \in \{n, n-1, \dots, n-k+1\}$  and  $\hat{g}^*$  denotes the same estimator as  $\hat{g}$  but based on the bootstrap functional pseudo-time series  $\mathcal{X}_1^*, \mathcal{X}_2^*, \dots, \mathcal{X}_n^*$ . The conditional (on  $\mathcal{X}_{n,k}$ ) distribution of the prediction error  $\mathcal{X}_{n+h} - \hat{\mathcal{X}}_{n+h}$  is then estimated using the conditional distribution of the bootstrap prediction error  $\mathcal{X}_{n+h}^* - \hat{\mathcal{X}}_{n+h}^*$ . We show that the described procedure leads to consistent estimates of the conditional distribution of interest. We also prove the consistency of the bootstrap in estimating the conditional distribution of the studentized prediction error process in  $\mathcal{H}$ . The latter consistency is important because it theoretically justifies the use of the proposed bootstrap method in the construction of simultaneous prediction bands for the  $h$ -step-ahead prediction that also appropriately account for the local variability of the corresponding prediction error. Using simulations and two empirical data applications the good finite sample performance of the bootstrap procedure proposed.

We perform dimension reduction via the truncation of the Karhunen-Loève representation and we capture the infinite-dimensional structure of the underlying functional process by allowing the number of principal components used to increase to infinite (at an appropriate rate) with  $n$ . These aspects of our procedure are common to the sieve-bootstrap introduced in Paparoditis (2018). However, apart from the differences in the technical tools used for establishing bootstrap validity, a novel, general backward autoregressive representation of the vector process of scores is introduced, which is a key part of the bootstrap procedure proposed in this paper. This representation allows for the generation of the functional pseudo time series  $\mathcal{X}_1^*, \mathcal{X}_2^*, \dots, \mathcal{X}_n^*$ , backward in time and enables, therefore, for this pseudo time series to satisfy the condition  $\mathcal{X}_t^* = \mathcal{X}_t$  for  $t \in \{n-k+1, n-k+2, \dots, n\}$ . The latter condition is essential for successfully evaluating the conditional distribution of the prediction error  $\mathcal{E}_{n+h} | \mathcal{X}_{n,k}$  using the bootstrap and for the construction of the desired prediction bands. The same condition, including the aforementioned backward vector autoregressive representation of the score process and the focus on prediction error distribution, also are the main differences to the resampling approach considered in Shang (2018) which has been used for estimating the long-run variance. This approach is based on bootstrapping the principal component scores by maximum entropy.

Antoniadis et al. (2006) and Antoniadis et al. (2016) considered nonparametric (kernel-type), one step ahead predictor and proposed a resampling method to construct pointwise prediction

intervals. Model-based bootstrap procedures to construct pointwise prediction intervals for one step ahead prediction under (mainly) FAR(1) model assumptions on the data generating process have been considered in [Raña et al. \(2016\)](#) and [Vilar et al. \(2018\)](#). These approaches differ from ours. They are developed for particular predictors, they are designed for pointwise prediction intervals only, and the bootstrap approaches involved, only are designed for the specific prediction setting considered. More related to our approach in terms of not requiring particular model assumptions for the data generating process and of not being designed for a specific predictor, is the approach proposed in [Aue et al. \(2015\)](#) for the construction of prediction bands. In Section 5 we compare the performance of this approach with the bootstrap approach proposed in this paper.

This paper is organized as follows. In Section 2, we state the notation used and introduce the notion of backward vector autoregressive representations of the time-reversed vector process of scores appearing in the Karhunen-Loève representation. In Section 3, we present the proposed bootstrap procedure and show its asymptotic validity for the construction of simultaneous prediction bands. Section 4 is devoted to some practical issues related to the construction of prediction bands and the implementation of our procedure. Section 5 investigates the finite sample performance of the proposed bootstrap procedure using simulations, while in Section 6, applications of the new methodology to a real-life data set are considered. Conclusions are provided in Section 7. The analysis of a second real-life data set as well as the proofs of the theoretical results presented in this paper together with some auxiliary lemmas are given in the Supplementary Material.

## 2 Preliminaries

### 2.1 Setup and Examples of Predictors

Consider a time series  $\mathcal{X}_1, \mathcal{X}_2, \dots, \mathcal{X}_n$  stemming from a stationary,  $L^4$ - $\mathcal{M}$ -approximable stochastic process  $\mathbf{X} = \{\mathcal{X}_t, t \in \mathbb{Z}\}$  with mean  $E(\mathcal{X}_t) = 0$  and autocovariance operator  $C_r = E(\mathcal{X}_t \otimes \mathcal{X}_{t+r})$ ,  $r \in \mathbb{Z}$ . Recall that  $C_r$  is a Hilbert-Schmidt (HS) operator. The  $L^4$ - $\mathcal{M}$  approximability property allows for a weak dependence structure of the underlying functional process, which covers a wide range of commonly used functional time series models, including functional linear processes and functional autoregressive, conditional heteroscedasticity processes; (see [Hörmann & Kokoszka 2010](#), for details).  $L^4$ - $\mathcal{M}$ -approximability implies that  $\sum_{r \in \mathbb{Z}} \|C_r\|_{\text{HS}} < \infty$  and therefore, that the

functional process  $\mathbf{X}$  possesses a continuous, self-adjoint spectral density operator  $\mathcal{F}_\omega$ , given by

$$\mathcal{F}_\omega = (2\pi)^{-1} \sum_{r \in \mathbb{Z}} C_r e^{-ir\omega}, \omega \in \mathbb{R},$$

which is trace class (Hörmann et al. 2015) (also see Panaretos & Tavakoli (2013) for a different set of weak dependence conditions on the functional process  $\mathbf{X}$ ). Here and in the sequel,  $\|\cdot\|_{HS}$  denotes the Hilbert-Schmidt norm of an operator while  $\|\cdot\|_F$  the Frobenious norm of a matrix. We assume that the eigenvalues  $\nu_1(\omega), \nu_2(\omega), \dots, \nu_m(\omega)$  of the spectral density operator  $\mathcal{F}_\omega$  are strictly positive for every  $\omega \in [0, \pi]$ .

Suppose that the  $h$ -step-ahead predictor of  $\mathcal{X}_{n+h}$  is obtained as

$$\hat{\mathcal{X}}_{n+h} = \hat{g}_{(h)}(\mathcal{X}_n, \dots, \mathcal{X}_{n-k+1}), \quad (5)$$

where  $k \in N$ ,  $k < n$ , is fixed and determined by the model selected to perform the prediction (see also (3)), while  $\hat{g}_{(h)}$  denotes an estimator of the unknown operator  $g_{(h)}$ . Based on  $\hat{\mathcal{X}}_{n+h}$ , our aim is to construct a prediction interval, respectively, prediction band for  $\mathcal{X}_{n+h}$  associated with the model (5) which is used for prediction. Toward this end, an estimator of the distribution of the prediction error  $\mathcal{E}_{n+h} = \mathcal{X}_{n+h} - \hat{\mathcal{X}}_{n+h}$  is needed. More precisely, we are interested in estimating the conditional distribution

$$\mathcal{E}_{n+h} | \mathcal{X}_n, \mathcal{X}_{n-1}, \dots, \mathcal{X}_{n-k+1}. \quad (6)$$

Since we do not want to restrict our considerations to a specific predictor  $\hat{g}$ , many of the predictors applied in the functional time series literature fit in our setup. We elaborate on some examples:

- 1) Suppose that in (3) the operator  $g$  is given by  $g(\mathcal{X}_n, \dots, \mathcal{X}_{n-k+1}) = \sum_{j=1}^k \Phi_j(\mathcal{X}_{n+1-j})$  with the  $\Phi_j$ 's being linear, bounded operators  $\Phi_j : \mathcal{H} \rightarrow \mathcal{H}$ . This is a case where a functional autoregressive model of order  $k$  (FAR( $k$ )) is used to predict  $\mathcal{X}_{n+h}$ , see (Kokoszka & Reimherr 2013b) in which the issue of the selection of the order  $k$  also is discussed. Given some estimators  $\hat{\Phi}_j$  of  $\Phi_j$ , the corresponding  $h$ -step-ahead predictor is given by  $\hat{g}(\hat{\mathcal{X}}_{n+h-1}, \dots, \hat{\mathcal{X}}_{n+h-k}) = \sum_{j=1}^k \hat{\Phi}_j(\hat{\mathcal{X}}_{n+h-j})$ , where  $\hat{\mathcal{X}}_t \equiv \mathcal{X}_t$  if  $t \in \{n, n-1, \dots, n-k+1\}$ . A special case is the popular FAR(1) model in which it is assumed that  $\mathcal{X}_t$  is generated as  $\mathcal{X}_t = \Phi(\mathcal{X}_{t-1}) + v_t$  with  $\|\Phi\|_{\mathcal{L}} < 1$  and  $v_t$  an i.i.d. sequence in  $\mathcal{H}$  (Bosq 2000, Bosq & Blanke 2007). Here and in the sequel,  $\|\cdot\|_{\mathcal{L}}$  denotes the operator norm.
- 2) Suppose that  $g_{(h)}(\mathcal{X}_n, \dots, \mathcal{X}_{n-k+1}) = \sum_{j=1}^d \mathbf{1}_j^\top \sum_{l=1}^k D_l \boldsymbol{\xi}_{n+h-l} v_j$ , where  $\mathbf{1}_j$  is the  $d$ -dimensional vector with the  $j^{\text{th}}$  component equal to 1 and 0 elsewhere,  $\boldsymbol{\xi}_t$  is the  $d$ -dimensional vector

$\boldsymbol{\xi}_t = (\langle \mathcal{X}_t, v_j \rangle, j = 1, 2, \dots, d)^\top$ ,  $v_j$  are the orthonormal eigenfunctions corresponding to the  $d$  largest eigenvalues of the lag-0 covariance operator  $C_0 = E(\mathcal{X}_0 \otimes \mathcal{X}_0)$ , and  $(D_1, D_2, \dots, D_k)$  are the matrices obtained by the orthogonal projection of  $\boldsymbol{\xi}_t$  on the space spanned by  $(\boldsymbol{\xi}_{t-1}, \boldsymbol{\xi}_{t-2}, \dots, \boldsymbol{\xi}_{t-k})$ . A predictor of  $\mathcal{X}_{n+h}$  is then obtained as

$$\hat{\mathcal{X}}_{n+h} = \sum_{j=1}^d \mathbf{1}_j^\top \check{\boldsymbol{\xi}}_{n+h} \hat{v}_j,$$

where  $\check{\boldsymbol{\xi}}_{n+h} = \sum_{l=1}^k \hat{D}_l \check{\boldsymbol{\xi}}_{n+h-l}$ ,  $\check{\boldsymbol{\xi}}_t = \hat{\boldsymbol{\xi}}_t$  for  $t \in \{n, n-1, \dots, n-k+1\}$  and  $\hat{\boldsymbol{\xi}}_1, \dots, \hat{\boldsymbol{\xi}}_n$  are the estimated  $d$ -dimensional score vectors  $\hat{\boldsymbol{\xi}}_t = (\langle \mathcal{X}_t, \hat{v}_j \rangle, j = 1, 2, \dots, d)^\top$ . Here  $\hat{v}_j$  are the estimated orthonormal eigenfunctions corresponding to the  $d$  largest estimated eigenvalues of  $\hat{\mathcal{C}}_0 = n^{-1} \sum_{t=1}^n (\mathcal{X}_t - \bar{\mathcal{X}}_n) \otimes (\mathcal{X}_t - \bar{\mathcal{X}}_n)$  and  $(\hat{D}_l, l = 1, 2, \dots, k)$  are the estimated  $d \times d$  matrices obtained by least squares fitting of a  $k^{\text{th}}$  order vector autoregression to the time series  $\hat{\boldsymbol{\xi}}_t, t = 1, 2, \dots, n$  (Aue et al. 2015).

- 3) Similar to 2), the predictor of  $\mathcal{X}_{n+h}$  can be obtained as  $\hat{\mathcal{X}}_{n+h} = \sum_{j=1}^d \mathbf{1}_j^\top \check{\boldsymbol{\xi}}_{n+h,j} \hat{v}_j$ , where  $\check{\boldsymbol{\xi}}_{n+h,j}$  is an  $h$ -step predictor of the  $j^{\text{th}}$  component, obtained via a univariate time series forecasting method applied to estimated components  $(\hat{\varepsilon}_{1,j}, \dots, \hat{\varepsilon}_{n,j})$  for each  $j = 1, \dots, d$ , (Hyndman & Shang 2009).
- 4) Let for notational simplicity  $k = 1$  and  $g_{(h)}(\mathcal{X}_n) = E(\mathcal{X}_{n+h} | \mathcal{X}_n)$  be the conditional mean function of  $\mathcal{X}_{n+h}$  given  $\mathcal{X}_n$ . Consider the predictor  $\hat{\mathcal{X}}_{n+h}$  obtained using a nonparametric estimator of  $g_{(h)}$ , for instance, a functional version of the Nadaraya-Watson estimator given by

$$\hat{g}_{(h)}(\mathcal{X}) = \sum_{i=1}^{n-h} \frac{K[d(\mathcal{X}_i, \mathcal{X})/\delta] \mathcal{X}_{i+h}}{\sum_{j=1}^{n-1} K[d(\mathcal{X}_j, \mathcal{X})/\delta]},$$

where  $K(\cdot)$  is a kernel function,  $\delta > 0$  is a smoothing bandwidth, and  $d(\cdot, \cdot)$  is a distance function on  $\mathcal{H}$ .  $\hat{\mathcal{X}}_{n+h} = \hat{g}_{(h)}(\mathcal{X}_n)$  is then the predictor of  $\mathcal{X}_{n+h}$ , (see, e.g., Antoniadis et al. 2006).

## 2.2 The Time-Reversed Process of Scores

To introduce the proposed bootstrap procedure, it is important to first discuss some properties of the time-reversed process of scores associated with the functional process  $\mathbf{X}$ . To this end, consider for  $m \in \mathbb{N}$ , the  $m$ -dimensional vector process of scores, that is  $\boldsymbol{\xi} = \{\boldsymbol{\xi}_t, t \in \mathbb{Z}\}$ , where

$\boldsymbol{\xi}_t = (\xi_{j,t} = \langle \mathcal{X}_t, v_j \rangle, j = 1, 2, \dots, m)^\top$  and  $v_1, v_2, \dots$ , are the orthonormal eigenvectors corresponding to the eigenvalues  $\lambda_1 > \lambda_2 > \dots$ , in descending order, of the lag-0 autocovariance operator  $C_0$ . Denote by  $\tilde{\boldsymbol{\xi}} = \{\tilde{\boldsymbol{\xi}}_t, t \in \mathbb{Z}\}$  the time-reversed version of  $\boldsymbol{\xi}$ , that is,  $\tilde{\boldsymbol{\xi}}_t = \boldsymbol{\xi}_{-t}$  for any  $t \in \mathbb{Z}$ . We call  $\boldsymbol{\xi}$  and  $\tilde{\boldsymbol{\xi}}$  the forward and the backward score processes, respectively. The autocovariance structure of both processes is closely related because for any  $h \in \mathbb{Z}$  we have

$$\begin{aligned} \Gamma_{\tilde{\boldsymbol{\xi}}}(h) &:= E \left[ \tilde{\boldsymbol{\xi}}_0(m) \tilde{\boldsymbol{\xi}}_h^\top(m) \right] \\ &= E \left[ \boldsymbol{\xi}_0(m) \boldsymbol{\xi}_{-h}^\top(m) \right] =: \Gamma_{\boldsymbol{\xi}}(-h). \end{aligned} \quad (7)$$

Thus, properties of the forward score process  $\boldsymbol{\xi}$ , which arise from its second-order structure, carry over to the backward process  $\tilde{\boldsymbol{\xi}}$ . To elaborate, note first that the (Hilbert-Schmidt) norm summability of the autocovariance operators  $C_h$  as well as the assumption that the eigenvalues  $\nu_1(\omega), \nu_2(\omega), \dots, \nu_m(\omega)$  of the spectral density operator  $\mathcal{F}_\omega$  are bounded away from zero for all  $\omega \in [0, \pi]$ , imply that, the  $m \times m$  spectral density matrix  $f_{\boldsymbol{\xi}}(\omega) = (2\pi)^{-1} \sum_{h \in \mathbb{Z}} \Gamma_{\boldsymbol{\xi}}(h) e^{-ih\omega}$  of the forward score process  $\boldsymbol{\xi}$ , is continuous, bounded from above and bounded away from zero from below; (see Lemma 2.1 of [Papadoditis 2018](#)). The same properties also hold true for the  $m \times m$  spectral density matrix  $f_{\tilde{\boldsymbol{\xi}}}(\omega) = (2\pi)^{-1} \sum_{h \in \mathbb{Z}} \Gamma_{\tilde{\boldsymbol{\xi}}}(h) e^{-ih\omega}$  of the backward score process  $\tilde{\boldsymbol{\xi}}$ . This follows immediately from the corresponding and aforementioned properties of  $f_{\boldsymbol{\xi}}$  and taking into account that by equation (7),  $f_{\tilde{\boldsymbol{\xi}}}(\omega) = f_{\boldsymbol{\xi}}^\top(\omega)$  for all  $\omega \in [0, \pi]$ . Now, the fact that both spectral density matrices  $f_{\boldsymbol{\xi}}$  and  $f_{\tilde{\boldsymbol{\xi}}}$  are bounded from above and from below, implies by Lemma 3.5 of [Cheng & Pourahmadi \(1993, p. 116\)](#), that both processes—the process  $\boldsymbol{\xi}$  and the time-reversed process  $\tilde{\boldsymbol{\xi}}$ —obey a so-called vector autoregressive representation. That is, infinite sequences of  $m \times m$  matrices  $\{A_j, j \in \mathbb{N}\}$  and  $\{B_j, j \in \mathbb{N}\}$  as well as full rank  $m$ -dimensional, white noise processes  $\{\mathbf{e}_t, t \in \mathbb{Z}\}$  and  $\{\mathbf{u}_t, t \in \mathbb{Z}\}$  exist such that the random vectors  $\boldsymbol{\xi}_t$  and  $\tilde{\boldsymbol{\xi}}_t$  have, respectively, the following autoregressive representations:

$$\boldsymbol{\xi}_t = \sum_{j=1}^{\infty} A_j \boldsymbol{\xi}_{t-j} + \mathbf{e}_t \quad (8)$$

and

$$\tilde{\boldsymbol{\xi}}_t = \sum_{j=1}^{\infty} B_j \tilde{\boldsymbol{\xi}}_{t-j} + \mathbf{u}_t. \quad (9)$$

We refer to (8) and (9) as the forward and backward vector autoregressive representations of  $\boldsymbol{\xi}_t$  and to  $\{\mathbf{e}_t\}$  and to  $\{\mathbf{u}_t\}$  as the forward and the backward noise processes. We stress here the fact that representations (8) and (9) should not be confused with that of a *linear* (infinite order) vector autoregressive process. This is due to the fact that the noise vector processes  $\{\mathbf{e}_t\}$  and  $\{\mathbf{u}_t\}$

appearing in representations (8) and (9), respectively, are only uncorrelated and not necessarily i.i.d. sequences of random vectors. Furthermore, the autoregressive matrices  $\{A_j\}$  and  $\{B_j\}$  appearing in the above representations also satisfy the summability conditions  $\sum_{j=1}^{\infty} \|A_j\|_F < \infty$  and  $\sum_{j=1}^{\infty} \|B_j\|_F < \infty$ , while the corresponding power series

$$A(z) = I - \sum_{j=1}^{\infty} A_j z^j \quad \text{and} \quad B(z) = I - \sum_{j=1}^{\infty} B_j z^j$$

do not vanish for  $|z| \leq 1$ ; that is,  $A^{-1}(z)$  and  $B^{-1}(z)$  exist for all  $|z| \leq 1$  (see [Cheng & Pourahmadi 1993](#), [Meyer & Kreiss 2015](#), for more details on such vector autoregressive representations of weakly stationary processes). Using reversion in time and, specifically, the property that  $\tilde{\xi}_t = \xi_{-t}$ , equation (9) leads to the expression

$$\xi_t = \sum_{j=1}^{\infty} B_j \xi_{t+j} + \mathbf{u}_t, \quad (10)$$

which also can be written as  $B(L^{-1})\xi_t = \mathbf{u}_t$ , with the shift operator  $L$  defined by  $L^k \xi_t = \xi_{t-k}$  for any  $k \in \mathbb{Z}$ . Expression (10) implies that the two white noise innovation processes  $\{\mathbf{e}_t, t \in \mathbb{Z}\}$  and  $\{\mathbf{u}_t, t \in \mathbb{Z}\}$ , are related by

$$\mathbf{u}_t = B(L^{-1})\xi_t = B(L^{-1})A^{-1}(L)\mathbf{e}_t, \quad t \in \mathbb{Z}. \quad (11)$$

Notice that (11) generalizes to the vector autoregressive case an analogue expression obtained for the univariate autoregressive case by [Findley \(1986\)](#) and [Breidt et al. \(1995\)](#). Further, and as relation (11) verifies, even if  $\xi_t$  in (8) is a linear process, that is even if  $\{\mathbf{e}_t\}$  is an i.i.d. innovation process in  $\mathbb{R}^m$ , the white noise innovation process  $\{\mathbf{u}_t\}$  appearing in the time-reversed process (10) is, in general, not an i.i.d. process.

## 3 Bootstrap Prediction Intervals

### 3.1 Bootstrap Procedure

The basic idea of the proposed bootstrap procedure is to generate a functional time series of pseudo-random elements  $\mathcal{X}_1^*, \mathcal{X}_2^*, \dots, \mathcal{X}_n^*$ , and future values  $\mathcal{X}_{n+1}^*, \mathcal{X}_{n+2}^*, \dots, \mathcal{X}_{n+h}^*$ , which appropriately imitate the dependence structure of the functional time series at hand, while at the same time satisfy the condition

$$\mathcal{X}_{n-k+1}^* = \mathcal{X}_{n-k+1}, \quad \mathcal{X}_{n-k+2}^* = \mathcal{X}_{n-k+2}, \quad \dots, \quad \mathcal{X}_n^* = \mathcal{X}_n. \quad (12)$$

The above condition is important because, as we have seen, the conditional distribution of  $\mathcal{E}_{n+1}(\cdot)$  given  $\mathcal{X}_n, \mathcal{X}_{n-1}, \dots, \mathcal{X}_{n-k+1}$  is the one in which we are interested. Toward this goal and motivated by the functional sieve bootstrap proposed by Paparoditis (2018), we use the Karhunen-Loève representation and decompose the random element  $\mathcal{X}_t$  in two parts:

$$\mathcal{X}_t = \sum_{j=1}^{\infty} \xi_{j,t} v_j = \underbrace{\sum_{j=1}^m \xi_{j,t} v_j}_{\mathcal{X}_{t,m}} + \underbrace{\sum_{j=m+1}^{\infty} \xi_{j,t} v_j}_{U_{t,m}}. \quad (13)$$

In (13), the element  $\mathcal{X}_{t,m}$  is considered as the main driving part of  $\mathcal{X}_t$ , while the “remainder”  $U_{t,m}$  is treated as a white noise component. Now, to generate the functional pseudo-time series  $\mathcal{X}_1^*, \mathcal{X}_2^*, \dots, \mathcal{X}_n^*$ , we first bootstrap the  $m$ -dimensional time series of scores by using the backward vector autoregressive representation given in (10). Using the backward representation allows for the generation of a pseudo-time series of scores  $\xi_1^*, \xi_2^*, \dots, \xi_n^*$ , which satisfies the condition  $\xi_t^* = \xi_t$  for  $t \in \{n-k+1, n-k+2, \dots, n\}$ . This is important to ensure that the bootstrap-generated time series  $\mathcal{X}_1^*, \mathcal{X}_2^*, \dots, \mathcal{X}_n^*$  fulfills requirement (12). The backwards-in-time-generated pseudo-time series of scores  $\xi_1^*, \xi_2^*, \dots, \xi_n^*$  can then be transformed to pseudo-replicates of the main driving part  $\mathcal{X}_{t,m}$  by using the equation  $\mathcal{X}_{t,m}^* = \sum_{j=1}^m \xi_{j,t}^* v_j$ . Notice that since by construction  $\xi_t^* = \xi_t$  for  $t = n, n-1, \dots, n-k+1$ , we have that  $\mathcal{X}_{t,m}^* = \mathcal{X}_{t,m}$  and, consequently, we set  $\mathcal{X}_t^* = \mathcal{X}_t$  for the same set of time indices. Adding to the generated  $\mathcal{X}_{t,m}^*$  for the remaining indices  $t = n-k, n-k-1, \dots, 1$ , an appropriately resampled functional noise  $U_{t,m}^*$ , leads to the functional pseudo replicates  $\mathcal{X}_1^*, \mathcal{X}_2^*, \dots, \mathcal{X}_{n-k}^*$ . As a result, a functional pseudo-time series  $\mathcal{X}_1^*, \mathcal{X}_2^*, \dots, \mathcal{X}_n^*$  can be obtained that imitates the dependence structure of  $\mathcal{X}_1, \mathcal{X}_2, \dots, \mathcal{X}_n$  and at the same time satisfies (12). Notice that implementation of the above ideas requires estimation of the eigenvectors  $v_j$  and of the scores  $\xi_{j,t} = \langle \mathcal{X}_t, v_j \rangle$ , because these quantities are not observed (see Section 3.2 for details).

Before proceeding with a precise description of the bootstrap algorithm, we illustrate its capability using a data example. Figure 1 shows the monthly sea surface temperatures for the last three years (analyzed in Section 6) together with 1,000 bootstrap replications obtained when  $k = 1$  and using the bootstrap algorithm described in Section 3.2. Notice the asymmetric features of the time series paths generated and the fact that all 1,000 bootstrap samples displayed pass through the same final curve. That is, all generated bootstrap functional time series satisfy condition (12), which for the case  $k = 1$  reduces to  $\mathcal{X}_n^* = \mathcal{X}_n$ .

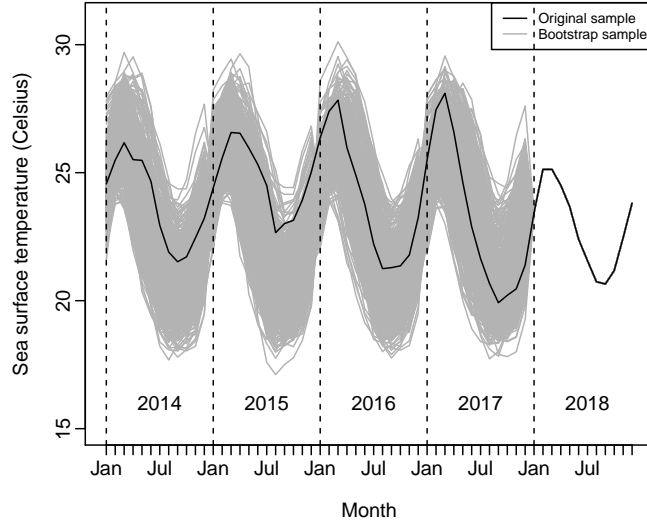


Figure 1: Sea surface temperature in El Niño region 1+2 displayed from January 2014 to December 2018 (black line) together with 1000 different bootstrap samples (gray lines) when  $k = 1$ .

### 3.2 Bootstrap Algorithm

We now proceed with a detailed description of the bootstrap algorithm used to generate the functional pseudo-time series  $\mathcal{X}_1^*, \mathcal{X}_2^*, \dots, \mathcal{X}_n^*$  and  $\mathcal{X}_{n+1}^*, \mathcal{X}_{n+2}^*, \dots, \mathcal{X}_{n+h}^*$ . Steps 1 to 3 of the following algorithm concern the generation of the future pseudo-elements  $\mathcal{X}_{n+1}^*, \mathcal{X}_{n+2}^*, \dots, \mathcal{X}_{n+h}^*$ , while Steps 4 to 6 the generation of  $\mathcal{X}_1^*, \dots, \mathcal{X}_n^*$ .

**Step 1:** Center the observed functional time series by calculating  $\mathcal{Y}_t = \mathcal{X}_t - \bar{\mathcal{X}}_n$ ,  $\bar{\mathcal{X}}_n = n^{-1} \sum_{t=1}^n \mathcal{X}_t$ .

**Step 2:** Select integers  $m$  and  $p$ , where  $m$  is the truncation number in (13) and  $p$  the order used to approximate the infinite-order vector autoregressive representations (8) and (9). Denote by  $\hat{\xi}_1, \hat{\xi}_2, \dots, \hat{\xi}_n$  the time series of estimated,  $m$ -dimensional vector of scores; that is,

$$\hat{\xi}_t = (\langle \mathcal{Y}_t, \hat{v}_j \rangle, j = 1, 2, \dots, m)^\top, t = 1, 2, \dots, n$$

where  $\hat{v}_j$ ,  $j = 1, 2, \dots, m$ , are the estimated (up to a sign) orthonormal eigenfunctions corresponding to the  $m$  largest estimated eigenvalues of the lag-0 sample autocovariance operator  $\hat{C}_0 = n^{-1} \sum_{t=1}^n \mathcal{Y}_t \otimes \mathcal{Y}_t$ .

**Step 3:** Fit a VAR( $p$ ) process to the “forward” series of estimated scores; that is,  $\hat{\xi}_t = \sum_{j=1}^p \hat{A}_{j,p} \hat{\xi}_{t-j} + \hat{e}_t$ ,  $t = p+1, p+2, \dots, n$ , with  $\hat{e}_t$  being the estimated residuals. Generate

$\boldsymbol{\xi}_{n+h}^* = \sum_{l=1}^p \hat{A}_{l,p} \boldsymbol{\xi}_{n+h-l}^* + \mathbf{e}_{n+h}^*$ , where we set  $\boldsymbol{\xi}_{n+h-l}^* = \hat{\boldsymbol{\xi}}_{n+h-l}$  if  $n+h-l \leq n$  and  $\mathbf{e}_{n+h}^*$  is i.i.d. resampled from the set of centered residuals  $\{\hat{\mathbf{e}}_t - \bar{\mathbf{e}}_n, t = p+1, p+2, \dots, n\}$ ,  $\bar{\mathbf{e}}_n = (n-p)^{-1} \sum_{t=p+1}^n \hat{\mathbf{e}}_t$ . Calculate

$$\mathcal{X}_{n+h}^* = \bar{\mathcal{X}}_n + \sum_{j=1}^m \mathbf{1}_j^\top \boldsymbol{\xi}_{n+h}^* \hat{v}_j + U_{n+h,m}^*,$$

where the  $U_{n+h,m}^*$  are i.i.d. resampled from the set  $\{\hat{U}_{t,m} - \bar{U}_n, t = 1, 2, \dots, n\}$ ,  $\bar{U}_n = n^{-1} \sum_{t=1}^n \hat{U}_{t,m}$  and  $\hat{U}_{t,m} = \mathcal{Y}_t - \sum_{j=1}^m \mathbf{1}_j^\top \hat{\boldsymbol{\xi}}_t \hat{v}_j$ . Recall that  $\mathbf{1}_j$  denotes the  $m$ -dimensional vector with the  $j^{\text{th}}$  component equal to 1 and 0 elsewhere.

If  $p \leq k+h$ , move to Step 4. If  $p > k+h$ , generate for  $l = 1, 2, \dots, p - (k+h)$  additional random vectors  $\boldsymbol{\xi}_{n+h+l}^* = \sum_{j=1}^p \hat{A}_{j,p} \boldsymbol{\xi}_{n+h+l-j}^* + \mathbf{e}_{n+h+l}^*$ , where  $\mathbf{e}_{n+h+l}^*$  are i.i.d. generated in the same way as  $\mathbf{e}_{n+h}^*$ .

**Step 4:** Fit a VAR( $p$ ) process to the “backward” series of estimated scores; that is,

$$\hat{\boldsymbol{\xi}}_t = \sum_{j=1}^p \hat{B}_{j,p} \hat{\boldsymbol{\xi}}_{t+j} + \hat{\mathbf{u}}_t, \quad t = 1, 2, \dots, n-p.$$

**Step 5:** Generate a pseudo-time series of the scores  $\{\boldsymbol{\xi}_1^*, \boldsymbol{\xi}_2^*, \dots, \boldsymbol{\xi}_n^*\}$  by setting  $\boldsymbol{\xi}_t^* = \hat{\boldsymbol{\xi}}_t$  for  $t = n, n-1, \dots, n-k+1$ , and by using for  $t = n-k, n-k-1, \dots, 1$ , the backward vector autoregression  $\boldsymbol{\xi}_t^* = \sum_{j=1}^p \hat{B}_{j,p} \boldsymbol{\xi}_{t+j}^* + \mathbf{u}_t^*$ . Here  $\mathbf{u}_1^*, \mathbf{u}_2^*, \dots, \mathbf{u}_{n-k}^*$  are obtained as (see (11)),

$$\mathbf{u}_t^* = \hat{B}_p(L^{-1}) \hat{A}_p^{-1}(L) \mathbf{e}_t^*,$$

with  $\hat{A}_p(z) = I - \sum_{j=1}^p \hat{A}_{j,p} z^j$ ,  $\hat{B}_p(z) = I - \sum_{j=1}^p \hat{B}_{j,p} z^j$ ,  $z \in \mathbb{C}$ , and where the  $\mathbf{e}_t^*$  are i.i.d. resampled as in Step 3.

**Step 6:** Generate a pseudo-functional time series  $\{\mathcal{X}_1^*, \mathcal{X}_2^*, \dots, \mathcal{X}_n^*\}$  as follows. For  $t = n, n-1, \dots, n-k+1$  set

$$\mathcal{X}_t^* = \bar{\mathcal{X}}_n + \sum_{j=1}^m \mathbf{1}_j^\top \hat{\boldsymbol{\xi}}_t \hat{v}_j + \hat{U}_{t,m} \equiv \mathcal{X}_t,$$

while for  $t = n-k, n-k-1, \dots, 1$ , use the obtained backward pseudo-scores  $\boldsymbol{\xi}_1^*, \boldsymbol{\xi}_2^*, \dots, \boldsymbol{\xi}_{n-k}^*$  and calculate

$$\mathcal{X}_t^* = \bar{\mathcal{X}}_n + \sum_{j=1}^m \mathbf{1}_j^\top \boldsymbol{\xi}_t^* \hat{v}_j + U_{t,m}^*.$$

Here, the  $U_{t,m}^*$  are i.i.d. pseudo-elements resampled as in Step 3.

**Step 7:** If model (3) is used to obtain the prediction  $\hat{\mathcal{X}}_{n+h}$ , then calculate the pseudo-predictor

$$\hat{\mathcal{X}}_{n+h}^* = \bar{\mathcal{X}}_n + \hat{g}^* \left( \hat{\mathcal{X}}_{n+h-1}^* - \bar{\mathcal{X}}_n^*, \hat{\mathcal{X}}_{n+h-2}^* - \bar{\mathcal{X}}_n^*, \dots, \hat{\mathcal{X}}_{n+h-k}^* - \bar{\mathcal{X}}_n^* \right), \quad (14)$$

where we set  $\hat{\mathcal{X}}_t^* - \bar{\mathcal{X}}_n^* \equiv \mathcal{X}_t - \bar{\mathcal{X}}_n$  for  $t = n, n-1, \dots, n-k+1$ ,  $\bar{\mathcal{X}}_n^* = n^{-1} \sum_{t=1}^n \mathcal{X}_t^*$  and  $\hat{g}^*$  is the same estimator as  $\hat{g}$  used in (4) but obtained using the generated pseudo-time series  $\mathcal{X}_1^*, \mathcal{X}_2^*, \dots, \mathcal{X}_n^*$ . Alternatively, the bootstrap analogue of (5) can be calculated as

$$\hat{\mathcal{X}}_{n+h}^* = \bar{\mathcal{X}}_n + \hat{g}_{(h)}^* (\mathcal{X}_n - \bar{\mathcal{X}}_n, \mathcal{X}_{n-1} - \bar{\mathcal{X}}_n, \dots, \mathcal{X}_{n-k+1} - \bar{\mathcal{X}}_n). \quad (15)$$

Here  $\hat{g}_{(h)}^*$  is the same estimator as  $\hat{g}_{(h)}$  given in (5) but based on the pseudo-time series  $\mathcal{X}_1^*, \mathcal{X}_2^*, \dots, \mathcal{X}_n^*$ .

**Step 8:** Use the distribution of  $\mathcal{E}_{n+h}^* = \mathcal{X}_{n+h}^* - \hat{\mathcal{X}}_{n+h}^*$  to approximate the (conditional) distribution of  $\mathcal{E}_{n+h} = \mathcal{X}_{n+h} - \hat{\mathcal{X}}_{n+h}$  given  $\mathcal{X}_{n-k+1}, \mathcal{X}_{n-k+2}, \dots, \mathcal{X}_n$ .

Before investigating the theoretical properties of the above bootstrap procedure and evaluating its practical implementation for the construction of prediction bands, some remarks are in order.

Notice that  $\mathcal{X}_{n+h}^*$  in Step 3 is generated in a model-free way, while the estimated model  $\hat{g}^*$  is only used for obtaining the pseudo-predictor  $\hat{\mathcal{X}}_{n+h}^*$ . In this way the pseudo-error  $\mathcal{X}_{n+h}^* - \hat{\mathcal{X}}_{n+h}^*$  is able to imitate not only the innovation and estimation errors affecting the prediction error  $\mathcal{X}_{n+h} - \hat{\mathcal{X}}_{n+h}$  but also the error arising from possible model misspecification. In Steps 4 and 5, the backward vector autoregressive representation is used to generate the pseudo time series of scores  $\xi_t^*$ ,  $t = 1, 2, \dots, n$ , where this pseudo time series satisfies the condition  $\xi_t^* = \hat{\xi}_t$  for  $t = n-k+1, n-k+2, \dots, n$ . This enables the generation of a functional pseudo-time series  $\mathcal{X}_1^*, \mathcal{X}_2^*, \dots, \mathcal{X}_n^*$  in Step 6, satisfying requirement (12). A problem occurs when  $p > k+h$ , that is, when the autoregressive order used is larger than the number of future functional observations needed to run the backward vector autoregression. In this case, the time series of scores must be extended with the  $p - (k+h)$  “missing” future scores. This problem is solved in Step 3 by generating the additional pseudo-scores  $\xi_{n+h+l}^*$ , for  $l = 1, 2, \dots, p - (k+h)$ .

### 3.3 Bootstrap Validity

We establish consistency of the proposed bootstrap procedure in approximating the conditional error distribution (6) of interest. Regarding the underlying class of functional processes, we assume that  $\mathbf{X}$  is a purely non-deterministic, mean square continuous and  $L^4$ - $\mathcal{M}$  approximable process.

The mean square continuity of  $\mathbf{X}$  implies that its mean and covariance functions are continuous. For simplicity of notation, we assume that  $E\mathcal{X}_t = 0$ .

Because we condition on the last  $k$  observations, in what follows, all asymptotic results are derived under the assumption that we have observed a functional time series  $\mathcal{X}_s, \mathcal{X}_{s+1}, \dots, \mathcal{X}_n$  in which we view  $n$  as fixed and allow  $s \rightarrow -\infty$ . This is also the meaning of the statement "as  $n \rightarrow \infty$ " used in all derivations and asymptotic considerations in the sequel. Some conditions regarding the underlying process  $\mathbf{X}$  and the behavior of the bootstrap parameters  $m$  and  $p$  as well as the estimators  $\hat{g}$  and  $\hat{g}^*$  used are first imposed. Notice that to achieve bootstrap consistency, it is necessary to allow for the order  $p$  of the fitted autoregression and the dimension  $m$  of the number of principal components used to increase to infinity with the sample size. This is required in order for the bootstrap to appropriately capture both the entire temporal dependence structure of the vector process of scores and the infinite-dimensional structure of the prediction error  $\mathcal{E}_{n+1}$ .

**Assumption 1:**

- (i) The autocovariance operator  $C_h$  of  $\mathbf{X}$  satisfies  $\sum_{h \in \mathbb{Z}} |h| \|C_h\|_{HS} < \infty$ .
- (ii) For all  $\omega \in [0, \pi]$ , the spectral density operator  $\mathcal{F}_\omega$  is of full rank, that is,  $\text{kern}(\mathcal{F}_\omega) = 0$  and the eigenvalues  $\lambda_j$  of the full rank covariance operator  $\mathcal{C}_0$  (in descending order) are denoted by  $\lambda_1 > \lambda_2 > \lambda_3 > \dots > 0$ .

**Assumption 2:** The sequences  $p = p(n)$  and  $m = m(n)$  satisfy  $p \rightarrow \infty$  and  $m \rightarrow \infty$ , as  $n \rightarrow \infty$ , such that

- (i)  $m^2/\sqrt{p} \rightarrow 0$ ,
- (ii)  $\frac{p^3}{\sqrt{nm}\lambda_m^2} \sqrt{\sum_{j=1}^m \alpha_j^{-2}} = O(1)$ , where  $\alpha_1 = \lambda_1 - \lambda_2$  and  $\alpha_j = \min\{\lambda_{j-1} - \lambda_j, \lambda_j - \lambda_{j+1}\}$  for  $j = 2, 3, \dots, m$ .
- (iii)  $m^4 p^2 \|\tilde{A}_{p,m} - A_{p,m}\|_F = O_P(1)$ , where  $\tilde{A}_{p,m} = (\tilde{A}_{1,p}, \tilde{A}_{2,p}, \dots, \tilde{A}_{p,p})$ , and  $A_{p,m} = (A_{1,p}, A_{2,p}, \dots, A_{p,p})$ . Here  $\tilde{A}_{j,p}, j = 1, 2, \dots, p$  are the same estimators as  $\hat{A}_{j,p}, j = 1, 2, \dots, p$ , but based on the time series of true scores  $\boldsymbol{\xi}_1, \boldsymbol{\xi}_2, \dots, \boldsymbol{\xi}_n$ . Furthermore,  $A_{j,p}, j = 1, 2, \dots, p$  are the coefficient matrices of the best (in the mean square sense) linear predictor of  $\boldsymbol{\xi}_t$  based on the finite past  $\boldsymbol{\xi}_{t-1}, \boldsymbol{\xi}_{t-2}, \dots, \boldsymbol{\xi}_{t-p}$ .

**Assumption 3:** The estimators  $\hat{g}$  and  $\hat{g}^*$  converge to the same limit  $g_0$ ; that is,  $\|\hat{g} - g_0\|_{\mathcal{L}} = o_P(1)$  and  $\|\hat{g}^* - g_0\|_{\mathcal{L}} = o_P(1)$ .

Several comments regarding the above assumptions are in order. Assumption 1(i) implies that the spectral density operator  $\mathcal{F}_\omega$  is a continuously differentiable function of the frequency  $\omega$ . Regarding Assumption 2, notice first that allowing for the number  $m$  of principal components used as well as the order  $p$  of the vector autoregression fitted to increase to infinity with the sample size, make the asymptotic analysis of the bootstrap quite involved. This is so because the bootstrap procedure is based on the time series of estimated instead of true scores, the dimension and the order of the fitted vector autoregression increase to infinity, and, at the same time, the eigenvalue  $\lambda_m$  of the lag zero covariance operator  $\mathcal{C}_0$ , approaches zero as  $m$  increases to infinity with  $n$ . As we will see, a slow increase of  $m$  and  $p$  with respect to  $n$  is required to balance these different effects.

To elaborate, parts (i) and (ii) of Assumption 2 summarize the conditions imposed on the rate of increase of  $m$  and  $p$  to establish bootstrap consistency. Before discussing these conditions in more detail, observe that Assumption 2(iii) is a condition that the estimators of the autoregressive coefficient matrices have to fulfill, after ignoring the effects caused by the fact that estimated instead of true scores are used. Observe first that in contrast to the estimators  $\hat{A}_{j,p}$ ,  $j = 1, 2, \dots, p$ , based on the vector of estimated scores  $\hat{\xi}_t$ , the estimators  $\tilde{A}_{j,p}$ ,  $j = 1, 2, \dots, p$ , stated in Assumption 2(iii) are based on the true (i.e., unobserved) vector of scores  $\xi_t$ ,  $t = 1, 2, \dots, n$ . As an example, consider the case where  $\tilde{A}_{j,p}$ ,  $j = 1, 2, \dots, p$ , are the well-known Yule-Walker estimators of  $A_{j,p}$ ,  $j = 1, 2, \dots, p$ . By the arguments given in Paparoditis (2018, p. 3521), we have in this case that  $\|\tilde{A}_{p,m} - A_{p,m}\|_F = O_P(mp(\sqrt{m}\lambda_m^{-1} + p)^2/\sqrt{n})$ . From this bound it is easily seen by straightforward calculations, that, for these estimators, Assumption 2(iii) is satisfied if  $m$  and  $p$  increase to infinity as  $n \rightarrow \infty$  slowly enough such that  $m^6 p^4 = O(\lambda_m^2 \sqrt{n})$  and  $p^2/m^2 = O(\sqrt{n})$ .

To give an example of a functional process, of an estimator  $\hat{A}_j$ ,  $j = 1, 2, \dots, p$  and of the rates with which  $p$  and  $m$  have to increase to infinity so that all parts of Assumption 2 are fulfilled, suppose again that Yule Walker estimators of  $A_{j,p}$ ,  $j = 1, 2, \dots, p$ , are used in the bootstrap procedure. Assume further that the eigenvalues of the lag zero covariance operator  $\mathcal{C}_0$  satisfy  $\lambda_j - \lambda_{j+1} \geq C \cdot j^{-\vartheta}$ ,  $j = 1, 2, \dots$ , where  $C$  is a positive constant and  $\vartheta > 1$ . That is, assume that the eigenvalues of the lag zero autocovariance operator  $\mathcal{C}_0$  converge at a polynomial rate to zero. As it is shown in the supplementary material, Assumption 2(i), (ii) and (iii) are then satisfied if  $p = O(n^\gamma)$  and  $m = O(n^\delta)$  with  $\gamma > 0$  and  $\delta > 0$ , such that

$$\gamma \in (0, 1/8) \text{ and } \delta \in (0, \delta_{max}), \text{ where } \delta_{max} = \min \left\{ \frac{1-6\gamma}{6\vartheta}, \frac{1-8\gamma}{12+4\vartheta}, \gamma/4 \right\}. \quad (16)$$

More specifically and if for instance,  $\vartheta = 2$ , then  $(1-8\gamma)/(12+4\vartheta) < (1-6\gamma)/6\vartheta$  and Assumption

2 is satisfied if

$$\gamma \in (0, 1/8) \quad \text{and} \quad \delta \in \left(0, \min \left\{ \frac{1-8\gamma}{20}, \gamma/4 \right\} \right).$$

Notice that  $0 < \gamma < 1/8$  ensures that  $(1 - 8\gamma)/20 > 0$ .

Concerning Assumption 3 and given that we do not focus on a specific predictor, this assumption is necessarily a high-level type assumption. It requires that the estimator  $\widehat{g}^*$ , which is based on the bootstrap pseudo-time series  $\mathcal{X}_1^*, \mathcal{X}_2^*, \dots, \mathcal{X}_n^*$ , converges in probability and in operator norm, to the same limit  $g_0$  as the estimator  $\widehat{g}$  based on the time series  $\mathcal{X}_1, \mathcal{X}_2, \dots, \mathcal{X}_n$ . Notice that Assumption 3 can only be verified in a case-by-case investigation for a specific operator  $g$  at hand and for the particular estimators  $\widehat{g}$  and  $\widehat{g}^*$  used to perform the prediction.

To elaborate, consider the following example. Suppose that a FAR(1) model  $\mathcal{X}_t = \Phi(\mathcal{X}_{t-1}) + \varepsilon_t$  is used in equations (5) and (14) to obtain the predictors  $\widehat{\mathcal{X}}_{n+1}$  and  $\widehat{\mathcal{X}}_{n+1}^*$ , respectively. A common estimator of  $\Phi$  based on an approximative solution of the Yule-Walker-type equation  $C_1 = \Phi C_0$ , is given by

$$\widehat{\Phi}_M(\cdot) = \frac{1}{n-1} \sum_{t=1}^{n-1} \sum_{i=1}^M \sum_{j=1}^M \frac{1}{\widehat{\lambda}_j} \langle \cdot, \widehat{v}_j \rangle \langle \mathcal{X}_t, \widehat{v}_j \rangle \langle \mathcal{X}_{t+1}, \widehat{v}_i \rangle \widehat{v}_i, \quad (17)$$

where  $M$  is some integer referring to the number of functional principal components included in the estimation of  $\Phi$  (Bosq 2000, Hörmann & Kokoszka 2012). Observe that (17) is a kernel operator with kernel

$$\widehat{\varphi}_M(\tau, \sigma) = \frac{1}{n-1} \sum_{t=1}^{n-1} \sum_{i=1}^M \sum_{j=1}^M \frac{1}{\widehat{\lambda}_j} \langle \mathcal{X}_t, \widehat{v}_j \rangle \langle \mathcal{X}_{t+1}, \widehat{v}_i \rangle \widehat{v}_j(\sigma) \widehat{v}_i(\tau) \quad (18)$$

and notice that  $\widehat{g} = \widehat{\Phi}_M$  in this example. Furthermore, for fixed  $M$  and by the consistency properties of  $\widehat{\lambda}_j$  and  $\widehat{v}_j$ , it is not difficult to show that  $\|\widehat{\Phi}_M(\cdot) - g_0\|_{\mathcal{L}} \xrightarrow{P} 0$ , where the limiting operator  $g_0$  is given by

$$g_0(\cdot) \equiv C_{1,M} \left( \sum_{j=1}^M \frac{1}{\lambda_j} \langle \cdot, v_j \rangle v_j \right). \quad (19)$$

Here,  $C_{1,M}(\cdot) = E\langle \mathcal{X}_{t,M}, \cdot \rangle \mathcal{X}_{t+1,M}$  is a finite rank approximation of the lag-1 autocovariance operator  $C_1$  (see equation (13) for the definition of  $\mathcal{X}_{t,M}$ ). Further,  $\sum_{j=1}^M \lambda_j^{-1} \langle \cdot, v_j \rangle v_j$  is the corresponding approximation of the inverse operator  $C_0^{-1}(\cdot) = \sum_{j=1}^{\infty} \lambda_j^{-1} \langle \cdot, v_j \rangle v_j$ , which appears when solving the aforementioned Yule-Walker-type equation (see Horváth & Kokoszka 2012, Chapter 13, for details). Similarly, the same convergence also holds true for the bootstrap estimator  $\widehat{g}_0^*$ , that is,  $\|\widehat{g}_0^* - g_0\|_{\mathcal{L}} \xrightarrow{P} 0$  with  $g_0$  given in (19). Now, if interest is focused on consistently estimating the operator  $\Phi$ , then, from an asymptotic perspective, the number  $M$  of functional principal components used in approximating the inverse of the operator  $C_0$ , has to increase to infinity at

an appropriate rate, as  $n$  goes to infinity. In this case, it can be shown under certain regularity conditions that  $\|\widehat{\Phi}_M - \Phi\|_{\mathcal{L}} = o_P(1)$  (see Bosq 2000, Theorem 8.7). Here  $g_0 = \Phi$ , and this limit is different from the one given in (19). In such a case, and for the estimator  $\widehat{g}^*$  to also converge to the same limit, additional arguments are needed since the technical derivations are then much more involved, compared to those used in the case of a fixed  $M$  (we refer to Paparoditis 2018, for more details on this type of asymptotic considerations).

Before stating our first consistency result, we fix some additional notation. Recall the definition of  $\mathcal{X}_{n,k}$  and denote by  $\mathcal{C}_{\mathcal{E},h}$  and  $\mathcal{C}_{\mathcal{E},h}^*$  the conditional covariance operators of the random elements  $\mathcal{E}_{n+h}$  and  $\mathcal{E}_{n+h}^*$ , respectively, given  $\mathcal{X}_{n,k}$ . That is,  $\mathcal{C}_{\mathcal{E},h} = E(\mathcal{E}_{n+h} \otimes \mathcal{E}_{n+h} | \mathcal{X}_{n,k})$  and  $\mathcal{C}_{\mathcal{E},h}^* = E^*(\mathcal{E}_{n+h}^* \otimes \mathcal{E}_{n+h}^* | \mathcal{X}_{n,k})$ , where  $E^*$  denotes expectation with respect to the bootstrap distribution. Recall that  $\mathcal{X}_t^* = \mathcal{X}_t$  for  $t \in \{n, n-1, \dots, n-k+1\}$ . Let further,

$$\sigma_{n+h}^2(\tau) = c_{\mathcal{E},h}(\tau, \tau) \quad \text{and} \quad \sigma_{n+h}^{*2}(\tau) = c_{\mathcal{E},h}^*(\tau, \tau), \quad \tau \in [0, 1],$$

where  $c_{\mathcal{E},h}$  and  $c_{\mathcal{E},h}^*$  denote the kernels of the conditional covariance (integral) operators  $\mathcal{C}_{\mathcal{E},h}$  and  $\mathcal{C}_{\mathcal{E},h}^*$ , respectively, which exist since these operators are Hilbert-Schmidt. Denote by  $\mathcal{L}_{\mathcal{X}_{n,k}}(\mathcal{E}_{n+h})$  the conditional distribution  $\mathcal{E}_{n+h} | \mathcal{X}_{n,k}$ , and by  $\mathcal{L}_{\mathcal{X}_{n,k}}(\mathcal{E}_{n+h}^* | \mathcal{X}_1, \mathcal{X}_2, \dots, \mathcal{X}_n)$  the conditional distribution  $\mathcal{E}_{n+h}^* | \mathcal{X}_{n,k}$ , given the observed functional time series  $\mathcal{X}_1, \mathcal{X}_2, \dots, \mathcal{X}_n$ . The following theorem establishes consistency of the bootstrap procedure in estimating the conditional distribution of interest.

**Theorem 3.1** *Suppose that Assumptions 1, 2, and 3 are satisfied. Then,*

$$d\left(\mathcal{L}_{\mathcal{X}_{n,k}}(\mathcal{E}_{n+h}), \mathcal{L}_{\mathcal{X}_{n,k}}(\mathcal{E}_{n+h}^* | \mathcal{X}_1, \mathcal{X}_2, \dots, \mathcal{X}_n)\right) = o_P(1), \quad (20)$$

where  $d$  is any metric metricizing weak convergence on  $\mathcal{H}$ .

The above result allows for the use of the conditional distribution of  $\mathcal{E}_{n+h}^*(\tau)$  to construct pointwise prediction intervals for  $\mathcal{X}_{n+h}(\tau)$ . Alternatively, consider the use of the conditional distribution of  $\sup_{\tau \in [0,1]} |\mathcal{E}_{n+h}^*(\tau)|$  to construct prediction bands for  $\mathcal{X}_{n+h}$ . Notice that the latter prediction bands will have the same width for all values of  $\tau \in [0, 1]$  since they do not appropriately reflect the local variability of the prediction error  $\mathcal{E}_{n+h}(\tau)$ . One way to take the (possible different) prediction uncertainty at every  $\tau \in [0, 1]$  into account, is to use the studentized conditional distribution of the prediction error, that is to use the process  $\{\mathcal{E}_{n+h}(\tau)/\sigma_{n+h}(\tau), \tau \in [0, 1]\}$  on  $\mathcal{H}$  in order to construct the prediction bands. However, in this case, and additional to the weak

convergence of  $\mathcal{E}_{n+h}^*$  to  $\mathcal{E}_{n+h}$  on  $\mathcal{H}$ , establishing bootstrap consistency requires the uniform (over  $\tau \in [0, 1]$ ) convergence of the conditional variance of the prediction error  $\sigma_{n+h}^{*2}(\tau)$  against  $\sigma_{n+h}^2(\tau)$ . This will allow for the proposed bootstrap procedure to appropriately approximate the random behavior of the studentized process  $\{\mathcal{E}_{n+h}(\tau)/\sigma_{n+h}(\tau), \tau \in [0, 1]\}$ . To achieve such a uniform consistency of bootstrap estimates, additional conditions compared to those stated in the previous Assumptions 2 and 3 are needed. We begin with the following modification of Assumption 2.

**Assumption 2':** The sequences  $m = m(n)$  and  $p = p(n)$  satisfy Assumptions 2 (i), (iii), and

(ii)  $\frac{p^5 m}{n^{1/2} \lambda_m^{5/2}} \sqrt{\sum_{j=1}^m \alpha_j^{-2}} = O(1)$ .

Our next assumption imposes additional conditions to those made in Assumption 3 and concern the mean square consistency properties of the estimators  $\widehat{g}_{(h)}$  and  $\widehat{g}_{(h)}^*$  used to perform the prediction.

**Assumption 3':** The estimators  $\widehat{g}_{(h)}(x)$  and  $\widehat{g}_{(h)}^*(x)$  satisfy for any given  $x \in \mathcal{H}^k$ ,  $\sup_{\tau \in [0, 1]} E|\widehat{g}_{(h)}(x)(\tau) - g_{0,h}(x)(\tau)|^2 \rightarrow 0$  and  $\sup_{\tau \in [0, 1]} E^*|\widehat{g}_{(h)}^*(x)(\tau) - g_{0,h}(x)(\tau)|^2 \rightarrow 0$  in probability.

The following proposition discusses the conditions that the initial estimators  $\widehat{g}$  and  $\widehat{g}^*$  have to fulfill so that Assumption 3' is satisfied for the important case where the limiting operator  $g_0$  is an integral operator. Recall that if  $g_0$  is an integral operator with kernel  $c_{g_0}$  satisfying  $\int_0^1 \int_0^1 |c_{g_0}(\tau, s)|^2 \tau ds < \infty$ , then  $g_0$  is also is a Hilbert-Schmidt operator.

**Proposition 3.1** *Suppose that  $g_0$  is an integral operator with kernel  $c_g : [0, 1] \times [0, 1] \rightarrow \mathbb{R}$  and let  $\widetilde{c}_g$  be an estimator of  $c_g$  and  $\widetilde{g}$  the corresponding integral operator. If  $\|\widetilde{g}\|_{HS}^2 \leq C$  for some constant  $C > 0$  and if*

$$(i) \quad E\|\widetilde{g} - g_0\|_{HS}^2 \rightarrow 0, \text{ and,}$$

$$(ii) \quad \sup_{\tau \in [0, 1]} E \int_0^1 (\widetilde{c}_g(\tau, s) - c_g(\tau, s))^2 ds \rightarrow 0,$$

as  $n \rightarrow \infty$ , then Assumption 3' is satisfied for any  $h \in \mathbb{N}$ .

We observe that apart from the basic requirement (i) on the mean square consistency of the estimator  $\widetilde{g}$  with respect to the Hilbert-Schmidt norm, the additional property one needs in case of integral operators is the uniform, mean square consistency stated in part (ii) of the above proposition. Bosq (2000, Theorem 8.7) established mean square consistency results when  $\widetilde{g} = \widehat{\Phi}_M$  with  $\widehat{\Phi}_M$  given in (17), in case  $g$  is an autoregressive, Hilbert-Schmidt operator of a FAR(1) process. Recall that in this case  $\|g\|_{HS}^2 = \int_0^1 \int_0^1 |c_{\widetilde{g}}(\tau, s)|^2 d\tau ds < 1$  is required in order to ensure stationarity

and causality of the FAR(1) process. Thus the requirement  $\|\tilde{g}\|_{HS}^2 \leq C$  stated in above proposition essentially means in this case, that the Hilbert-Schmidt norm of the estimator  $\tilde{g}$  used, should be bounded away from unity, uniformly in  $n$ .

We now establish the next theorem, which concerns the weak convergence of  $\mathcal{L}_{\mathcal{X}_{n,k}}(\mathcal{E}_{n+h}^*)$  as well as the uniform convergence of the conditional variance function  $\sigma_{n+h}^{*2}(\cdot)$  of the bootstrap prediction error.

**Theorem 3.2** *Suppose that Assumption 1,  $\mathcal{J}'$  and  $\mathcal{J}$  are satisfied. Then, additional to assertion (20) of Theorem 3.1, the following also holds true:*

$$\sup_{\tau \in [0,1]} \left| \sigma_{n+h}^{*2}(\tau) - \sigma_{n+h}^2(\tau) \right| \rightarrow 0, \quad \text{in probability.} \quad (21)$$

Theorem 3.2 and Slutsky's theorem theoretically justify the use of  $\{\mathcal{E}_{n+h}^*(\tau) / \sigma_{n+h}^*(\tau), \tau \in [0, 1]\}$  to approximate the behavior of  $\{\mathcal{E}_{n+h}(\tau) / \sigma_{n+h}(\tau), \tau \in [0, 1]\}$ . As the following corollary shows, the bootstrap can then successfully be applied to construct a simultaneous prediction band for  $\mathcal{X}_{n+h}$  that appropriately takes into account the local uncertainty of prediction.

**Corollary 3.1** *Suppose that the assumptions of Theorem 3.2 are satisfied. For  $\tau \in [0, 1]$ , let*

$$V_{n+h}(\tau) = \frac{\mathcal{X}_{n+h}(\tau) - \hat{\mathcal{X}}_{n+h}(\tau)}{\sigma_{n+h}(\tau)}, \quad \text{and} \quad V_{n+h}^*(\tau) = \frac{\mathcal{X}_{n+h}^*(\tau) - \hat{\mathcal{X}}_{n+h}^*(\tau)}{\sigma_{n+h}^*(\tau)}.$$

Then,

$$\sup_{x \in \mathbb{R}} \left| P \left( \sup_{\tau \in [0,1]} |V_{n+h}(\tau)| \leq x \mid \mathcal{X}_{n,k} \right) - P^* \left( \sup_{\tau \in [0,1]} |V_{n+h}^*(\tau)| \leq x \mid \mathcal{X}_{n,k} \right) \right| \rightarrow 0,$$

in probability, where  $P^*(A)$  denotes the probability of the event  $A$  given the functional time series  $\mathcal{X}_1, \mathcal{X}_2, \dots, \mathcal{X}_n$ .

## 4 Practical Construction of Prediction Intervals

As mentioned, the theoretical results of the previous section allow for the use of the quantiles of the distribution of  $\mathcal{E}_{n+h}^*(\tau)$ , or of  $V_{n+h}^*(\tau)$ , to construct either pointwise prediction intervals for  $\mathcal{X}_{n+h}(\tau)$  for any  $\tau \in [0, 1]$ , or simultaneous prediction bands for  $\{\mathcal{X}_{n+h}(\tau), \tau \in [a, b]\}$  for any  $0 \leq a < b \leq 1$ . Notice that the conditional distributions of  $\mathcal{E}_{n+h}^*(\tau)$  and  $V_{n+h}^*(\tau)$  can be evaluated by Monte Carlo, that is, by generating  $B$  replicates of  $\mathcal{E}_{n+h}^*$  and  $\sigma_{n+h}^*$ , say,  $\mathcal{E}_{n+h,1}^*, \mathcal{E}_{n+h,2}^*, \dots, \mathcal{E}_{n+h,B}^*$  and  $\sigma_{n+h,1}^*, \sigma_{n+h,2}^*, \dots, \sigma_{n+h,B}^*$ . Let  $M_{n,h}^* = \sup_{\tau \in [a,b]} |V_{n+h}^*(\tau)|$ , where  $V_{n+h}^*(\tau) = \mathcal{E}_{n+h}^*(\tau) / \sigma_{n+h}^*(\tau)$ , and denote by  $Q_{h,1-\alpha}^*$  the  $1 - \alpha$  quantile of the distribution of  $M_{n,h}^*$ . This distribution can

consistently be estimated using the  $B$  replicates,  $V_{n+h,b}^*(\tau) = \mathcal{E}_{n+h,b}^*(\tau)/\sigma_{n+h,b}^*(\tau)$ ,  $b = 1, 2, \dots, B$ . The simultaneous  $(1 - \alpha)100\%$  prediction band for  $\mathcal{X}_{n+h}$  over the desired interval  $[a, b]$ , associated with the predictor  $\widehat{\mathcal{X}}_{n+h}$ , is then given by

$$\left\{ [\widehat{\mathcal{X}}_{n+h}(\tau) - Q_{h,1-\alpha}^* \cdot \sigma_{n+h}^*(\tau), \widehat{\mathcal{X}}_{n+h}(\tau) + Q_{h,1-\alpha}^* \cdot \sigma_{n+h}^*(\tau)], \quad \tau \in [a, b] \right\}. \quad (22)$$

Clearly, a pointwise prediction interval for and any  $\tau \in [0, 1]$ , or a prediction band for the entire interval  $[0, 1]$ , can be obtained as special cases of (22). By the theoretical results established in Section 3, this prediction band achieves (asymptotically) the desired coverage probability  $1 - \alpha$ .

## 5 Simulations

### 5.1 Choice of Tuning Parameters

The theory developed in Section 3 formulates conditions on the rates at which the bootstrap tuning parameters  $m$  and  $p$  have to increase to infinity with the sample size  $n$  such that bootstrap consistency can be established. An optimal choice of these parameters in practice, which also is consistent with the theoretical requirements stated in Section 3.3, is left as an open problem for future research. In this section, we will discuss some relatively simple and practical rules to select  $m$  and  $p$ , which we found to work well in practice.

We first mention that different approaches have been proposed in the literature on how to choose  $m$  and that these approaches also can be applied in our setting. We mention here, among others, the pseudo-versions of the Akaike information criterion and Bayesian information criterion considered in (Yao et al. 2005); the finite prediction error criterion considered in (Aue et al. 2015); the eigenvalue ratio tests (Ahn & Horenstein 2013) and the generalized variance ratio criterion introduced in (Paparoditis 2018). However, and in order to reduce the computational burden in our simulation experiments, we apply a simple and commonly used rule to select the number  $m$  of functional principal components. This parameter is chosen here using the ratio of the variance explained by the  $m$  principal components to the total variance of the random element  $\mathcal{X}_t$ . More specifically,  $m$  is selected as

$$m_{n,Q} = \operatorname{argmin}_{m \geq 1} \left\{ \frac{\sum_{j=1}^m \widehat{\lambda}_j}{\sum_{j=1}^n \widehat{\lambda}_j} \geq Q \right\},$$

where  $\widehat{\lambda}_s$  denotes the  $s^{\text{th}}$  estimated eigenvalue of the sample lag-0 covariance operator  $\widehat{\mathcal{C}}_0$ , and  $Q$  is a pre-determined value, with  $Q = 0.85$  being a common choice (see, e.g., Hörmann & Kokoszka

2012, p.41). Once the parameter  $m$  has been selected, the order  $p$  of the fitted VAR model is chosen using a corrected Akaike information criterion (Hurvich & Tsai 1993), that is, by minimizing

$$\text{AICC}(p) = n \log \left| \widehat{\Sigma}_{e,p} \right| + \frac{n(nm + pm^2)}{n - m(p + 1) - 1},$$

over a range of values of  $p$ . Here  $\widehat{\Sigma}_{e,p} = n^{-1} \sum_{t=p+1}^n \widehat{\mathbf{e}}_{t,p} \widehat{\mathbf{e}}_{t,p}^\top$  and  $\widehat{\mathbf{e}}_{t,p}$  are the residuals obtained by fitting the VAR( $p$ ) model to the  $m$ -dimensional, vector time series of estimated scores,  $\widehat{\xi}_1, \widehat{\xi}_2, \dots, \widehat{\xi}_n$ ; see also Step 3 of the bootstrap algorithm.

## 5.2 Simulation Study

We utilize Monte Carlo methods to investigate the finite sample performance of the proposed bootstrap procedure. In particular, the final goal of our simulation study is to evaluate the interval forecast accuracy of the bootstrap prediction intervals under both regimes, that is, when the model used for prediction coincides with the model generating the data and when this is not the case. To this end, and in the first part of our simulation experiment, we always use a FAR(1) model for prediction. At the same time, we consider a data generating process, which allows for the investigation of the behavior of the proposed bootstrap procedure to construct prediction bands under both aforementioned regimes. The functional time series  $\mathcal{X}_1, \mathcal{X}_2, \dots, \mathcal{X}_n$  used stems from the process

$$\mathcal{X}_t(\tau) = \int_0^1 \psi(\tau, s) \mathcal{X}_{t-1}(s) ds + b \cdot \mathcal{X}_{t-2}(\tau) + B_t(\tau) + c \cdot B_{t-1}(\tau), \quad t = 1, 2, \dots, n, \quad (23)$$

where  $\psi(\tau, s) = 0.34 \exp^{\frac{1}{2}(\tau^2 + s^2)}$ ,  $\tau \in [0, 1]$ , and  $B_t(\tau)$  are Brownian motions with zero mean and variance  $1/(L - 1)$  with  $L = n + 1$ . Notice that  $\|\Psi\|_{\mathcal{L}} \approx 0.5$ , where  $\Psi$  is the integral operator associated with the kernel  $\psi$ . Three parameter combinations are considered:

**Case I:**  $b = c = 0$ ;      **Case II:**  $b = 0.4$  and  $c = 0$ ;      **Case III:**  $b = 0.4$  and  $c = 0.8$ .

Notice that for  $b = c = 0$ , the data are generated by a FAR(1) model, so in this case, the model used for prediction coincides with the model generating the functional time series. In Case II and for  $b = 0.4$  and  $c = 0$ , the data generating process follows a FAR(2) model, which is stationary because  $\|\Psi\|_{\mathcal{L}} + |b| < 1$ . This case imitates a regime of model misspecification. A situation of an even “heavier” model misspecification is simulated in Case III, where for  $b = 0.4$  and  $c = 0.8$ , the data generating process is a stationary FARMA(2,1) process with a large moving average component.

Four sample sizes are considered in the simulation study,  $n = 100, 200, 400$  and  $800$ . Using the first 80% of the data as the initial training sample, we compute a one-step-ahead prediction interval. Then, we increase the training sample by one and compute the one-step-ahead prediction interval again. This procedure continues until the training sample reaches the sample size. With 20% of the data as the testing sample, we compute the interval forecast accuracy of the one-step-ahead prediction based on the FAR(1) model used for prediction. We present results evaluating the performance of the bootstrap method for all three cases described above.

In the second part of our simulation experiment, we compare the finite sample performance of the bootstrap for constructing simultaneous prediction bands with that of the procedure proposed as Algorithm 4 in [Aue et al. \(2015, Section 5.2\)](#). In this comparison, the full FARMA(2,1) model is used to generate the data, that is, model (23) with  $b = 0.4$  and  $c = 0.8$ . At the same time, the one-step-ahead predictor  $\hat{\mathcal{X}}_{n+1}$  is obtained using the prediction method proposed by the authors in the [aforecited paper](#). See also case 2) in Section 2.1.

### 5.3 Evaluation Criteria of the Interval Forecast Accuracy

To measure the interval forecast accuracy, we consider the coverage probability difference (CPD) between the nominal coverage probability and empirical coverage probability and the interval score criterion of [Gneiting & Raftery \(2007\)](#). The pointwise and uniform empirical coverage probabilities are defined as

$$\begin{aligned} \text{Coverage}_{\text{pointwise}} &= 1 - \frac{1}{n_{\text{test}} \times J} \sum_{\eta=1}^{n_{\text{test}}} \sum_{j=1}^J \left[ \mathbb{1}\{\mathcal{X}_{\eta}(\tau_j) > \hat{\mathcal{X}}_{\eta}^{\text{ub}}(\tau_j)\} + \mathbb{1}\{\mathcal{X}_{\eta}(\tau_j) < \hat{\mathcal{X}}_{\eta}^{\text{lb}}(\tau_j)\} \right], \\ \text{Coverage}_{\text{uniform}} &= 1 - \frac{1}{n_{\text{test}}} \sum_{\eta=1}^{n_{\text{test}}} [\mathbb{1}\{\mathcal{X}_{\eta}(\tau) > \hat{\mathcal{X}}_{\eta}^{\text{ub}}(\tau)\} + \mathbb{1}\{\mathcal{X}_{\eta}(\tau) < \hat{\mathcal{X}}_{\eta}^{\text{lb}}(\tau)\}], \end{aligned}$$

where  $n_{\text{test}}$  denotes the number of curves in the forecasting period,  $J$  denotes the number of discretized data points,  $\hat{\mathcal{X}}_{\eta}^{\text{ub}}$  and  $\hat{\mathcal{X}}_{\eta}^{\text{lb}}$  denote the upper and lower bounds of the corresponding prediction interval, and  $\mathbb{1}\{\cdot\}$  the indicator function. The pointwise and uniform CPDs are defined as

$$\begin{aligned} \text{CPD}_{\text{pointwise}} &= |\text{Coverage}_{\text{pointwise}} - \text{Nominal coverage}| \\ \text{CPD}_{\text{uniform}} &= |\text{Coverage}_{\text{uniform}} - \text{Nominal coverage}|. \end{aligned}$$

Clearly, the smaller the CPD value, the better the performance of the forecasting method.

The mean interval score criterion introduced by [Gneiting & Raftery \(2007\)](#), is denoted by  $\overline{S}_\alpha$  and combines both CPD and half-width of pointwise prediction interval. It is defined as

$$\begin{aligned} \overline{S}_\alpha = \frac{1}{n_{\text{test}} \times J} \sum_{\eta=1}^{n_{\text{test}}} \sum_{j=1}^J \left\{ \left[ \hat{\mathcal{X}}_\eta^{\text{ub}}(\tau_j) - \hat{\mathcal{X}}_\eta^{\text{lb}}(\tau_j) \right] + \frac{2}{\alpha} \left[ \mathcal{X}_\eta(\tau_j) - \hat{\mathcal{X}}_\eta^{\text{ub}}(\tau_j) \right] \mathbb{1} \left[ \mathcal{X}_\eta(\tau_j) > \hat{\mathcal{X}}_\eta^{\text{ub}}(\tau_j) \right] \right. \\ \left. + \frac{2}{\alpha} \left[ \hat{\mathcal{X}}_\eta^{\text{lb}}(\tau_j) - \mathcal{X}_\eta(\tau_j) \right] \mathbb{1} \left[ \mathcal{X}_\eta(\tau_j) < \hat{\mathcal{X}}_\eta^{\text{lb}}(\tau_j) \right] \right\}, \end{aligned}$$

where  $\alpha$  denotes the level of coverage, customarily  $\alpha = 0.2$  corresponding to 80% prediction interval and  $\alpha = 0.05$  corresponding to 95% prediction interval. The optimal interval score is achieved when  $\mathcal{X}_\eta(\tau_j)$  lies between  $\hat{\mathcal{X}}_\eta^{\text{lb}}(\tau_j)$  and  $\hat{\mathcal{X}}_\eta^{\text{ub}}(\tau_j)$ , with the distance between the upper bound and lower bounds being minimal.

## 5.4 Simulation Results

As already mentioned, in the first part of our simulations, we use an estimated FAR(1) model to perform the prediction. The corresponding FAR(1) predictor is obtained as  $\hat{\mathcal{X}}_{n+1} = \overline{\mathcal{X}}_n + \hat{\Phi}(\mathcal{X}_n - \overline{\mathcal{X}}_n)$ , where  $\hat{\Phi}$  is a regularized, Yule-Walker-type estimator; see also (17). Table 1 and Table 2 present results based on 1,000 replications (i.e., a pseudo-random seed for each replication) and  $B = 1,000$  bootstrap repetitions. For the case  $n = 800$  and for computational reasons, we only consider 300 replications. Table 1 presents results for Case I ( $b = c = 0$ ) and Case II ( $b = 0.4, c = 0$ ) while Table 2 for Case III ( $b = 0.4, c = 0.8$ ).

From Table 1 and Table 2 some interesting observations can be made. First of all, the empirical coverage of the prediction intervals is good, even for the small sample sizes considered. It improves fast and considerably as the sample size increases, and they get quite close to the desired nominal coverages. This is true for both the pointwise prediction intervals and the simultaneous prediction bands considered and for both coverage levels used in the simulation study. Further, the  $\overline{S}_\alpha$  values are systematically larger for the cases  $b = 0.4, c = 0$  and  $b = 0.4, c = 0.8$  than for the case  $b = c = 0$ . As discussed in the introduction, this expected result is attributable to the fact that the model misspecification errors occurring for  $b = 0.4$  and  $c = 0.8$ , respectively, for  $b = 0.4$  and  $c = 0$ , also cause an increase in the variability of the prediction error distribution, leading to prediction intervals that are wider than those for  $b = 0$  and  $c = 0$ . Consequently, for the “heavier” case of model misspecification, Case III, that is for  $b = 0.4$  and  $c = 0.8$ , the  $\overline{S}_\alpha$  values are larger than for the case  $b = 0.4$  and  $c = 0$ .

We next present in Table 3 results for the second part of our simulations, which compare the performance of the bootstrap method proposed in this paper with Algorithm 4 in [Aue et al. \(2015\)](#)

Table 1: Empirical performance of the bootstrap prediction intervals and bands using the FAR(1) model to perform one-step-ahead predictions for functional time series stemming from model (23) with  $c = 0$  and for Case I ( $b = 0$ ) and Case II ( $b = 0.4$ ).

Nominal		$n = 100$		$n = 200$		$n = 400$		$n = 800$	
coverage	Criterion	$b = 0$	$b = 0.4$	$b = 0$	$b = 0.4$	$b = 0$	$b = 0.4$	$b = 0$	$b = 0.4$
80%	Coverage <sub>pointwise</sub>	0.778	0.745	0.791	0.778	0.797	0.797	0.799	0.797
	CPD <sub>pointwise</sub>	0.0497	0.0739	0.0344	0.0413	0.0230	0.0238	0.0167	0.0180
	Coverage <sub>uniform</sub>	0.772	0.714	0.798	0.766	0.812	0.792	0.803	0.796
	CPD <sub>uniform</sub>	0.0841	0.1152	0.0551	0.0647	0.0390	0.0391	0.0271	0.0283
	$\bar{S}_{\alpha=0.2}$	2.5322	2.9329	2.5346	2.7687	2.4764	2.6647	2.4398	2.6141
95%	Coverage <sub>pointwise</sub>	0.925	0.897	0.932	0.919	0.936	0.930	0.943	0.940
	CPD <sub>pointwise</sub>	0.0344	0.0580	0.0245	0.0344	0.0172	0.0220	0.0164	0.0202
	Coverage <sub>uniform</sub>	0.920	0.877	0.932	0.909	0.941	0.927	0.946	0.934
	CPD <sub>uniform</sub>	0.0516	0.0862	0.0338	0.0502	0.0230	0.0303	0.0185	0.0282
	$\bar{S}_{\alpha=0.05}$	3.4949	4.3379	3.5005	3.9347	3.3988	3.7328	3.3558	3.6646

Table 2: Empirical performance of the bootstrap prediction intervals and bands using the FAR(1) model to perform one-step-ahead predictions for functional time series stemming from model (23) with  $b = 0.4$  and  $c = 0.8$ .

Nominal		$n = 100$	$n = 200$	$n = 400$	$n = 800$
coverage	Criterion				
80%	Coverage <sub>pointwise</sub>	0.741	0.782	0.803	0.820
	CPD <sub>pointwise</sub>	0.0888	0.0467	0.0275	0.0235
	Coverage <sub>uniform</sub>	0.735	0.793	0.827	0.853
	CPD <sub>uniform</sub>	0.1164	0.0652	0.0469	0.0542
	$\bar{S}_{\alpha=0.2}$	3.5907	3.0588	2.8808	2.7326
95%	Coverage <sub>pointwise</sub>	0.890	0.919	0.931	0.942
	CPD <sub>pointwise</sub>	0.0702	0.0372	0.0220	0.0114
	Coverage <sub>uniform</sub>	0.875	0.914	0.934	0.950
	CPD <sub>uniform</sub>	0.0921	0.0484	0.0271	0.0142
	$\bar{S}_{\alpha=0.05}$	5.8624	4.4679	4.0899	3.8067

and used to construct one-step-ahead prediction bands. Notice that the predictor  $\hat{\mathcal{X}}_{n+1}$  used in this part of the simulation study is the one proposed in [Aue et al. \(2015\)](#). As it is seen from Table 3, the bootstrap approach proposed outperforms the aforementioned algorithm in [Aue et al. \(2015\)](#), in that the coverage rates are uniformly closer to the nominal levels and the mean interval scores  $\bar{S}_\alpha$ , are smaller for all  $\alpha$  and for both sample sizes considered.

Table 3: Finite sample performance of the bootstrap prediction intervals and of the prediction intervals of [Aue et al. \(2015\)](#) for time series stemming from model (23) with  $b = 0.4$  and  $c = 0.8$ .

Nominal		$n = 100$		$n = 200$	
coverage	Criterion	<a href="#">Aue et al.'s (2015)</a>	Bootstrap	<a href="#">Aue et al.'s (2015)</a>	Bootstrap
80%	Coverage <sub>pointwise</sub>	0.911	0.837	0.880	0.833
	CPD <sub>pointwise</sub>	0.1140	0.0610	0.0901	0.0348
	Coverage <sub>uniform</sub>	0.915	0.842	0.884	0.824
	CPD <sub>uniform</sub>	0.1255	0.0897	0.0921	0.0466
	$\bar{S}_{\alpha=0.2}$	6.0432	3.0487	5.4047	2.7993
95%	Coverage <sub>pointwise</sub>	0.977	0.953	0.967	0.949
	CPD <sub>pointwise</sub>	0.0340	0.0291	0.0235	0.0106
	Coverage <sub>uniform</sub>	0.974	0.946	0.968	0.949
	CPD <sub>uniform</sub>	0.0400	0.0435	0.0240	0.0154
	$\bar{S}_{\alpha=0.05}$	7.1303	4.3025	5.7686	3.8679

## 6 Empirical Data Analysis

For the two real-life data sets analyzed in this section and in the supplementary material, we consider (one and two step head) prediction using a FAR(1) model and a nonparametric forecasting method (NFR). The latter method applied for one-step-ahead prediction, uses a nonparametric estimation of the lag-1 conditional mean function  $g(\mathcal{X}_n) = E(\mathcal{X}_{n+1}|\mathcal{X}_n)$  (also see Section 2.1). Recall that  $g(\mathcal{X}_n)$  is the best (in the mean square sense) predictor of  $\mathcal{X}_{n+1}$  based on  $\mathcal{X}_n$ , and that different data-driven smoothing techniques exist for estimation of  $g$ . We refer to the functional

Nadaraya-Watson estimator (see, e.g., [Masry 2005](#), [Ferraty & Vieu 2006](#)), the functional local linear estimator, [Berlinet et al. \(2011\)](#), the functional  $k$ -nearest neighbor estimator, [Kudraszow & Vieu \(2013\)](#), and the distance-based local linear estimator [Boj et al. \(2010\)](#), to name a few. We use for the one-step-ahead prediction the Nadaraya-Watson estimator of  $g$ , which leads to the predictor  $\hat{\mathcal{X}}_{n+1} = \hat{g}(\mathcal{X}_n)$  with  $\hat{g}$  given by

$$\hat{g}(x) = \frac{\sum_{t=2}^n K(d(x, \mathcal{X}_{t-1})/\delta) \mathcal{X}_t}{\sum_{t=2}^n K(d(x, \mathcal{X}_{t-1})/\delta)}.$$

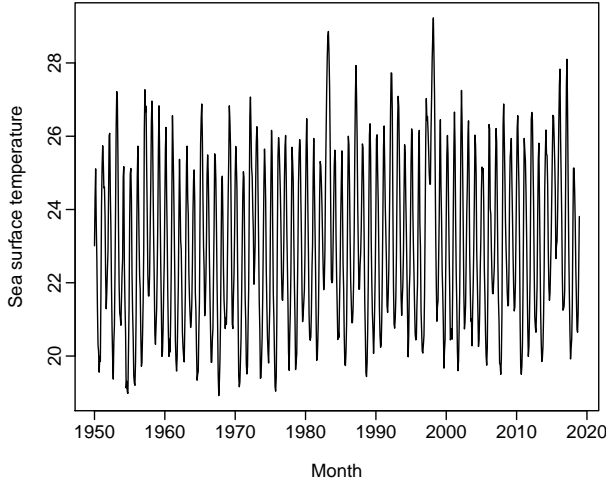
In the Nadaraya-Watson estimator,  $K(\cdot)$  is the Gaussian kernel and  $\delta$  is bandwidth, which in our calculations has been obtained using a generalized cross-validation procedure.

In addition to the construction of prediction bands, we also demonstrate how the proposed bootstrap method can be used to select the prediction method that performs better according to some user-specified criterion. In particular, since the future random element  $\mathcal{X}_{n+1}^*$  is generated in a model-free way, the bootstrap prediction error  $\hat{\mathcal{X}}_{n+1}^* - \mathcal{X}_{n+1}^*$  correctly imitates the behavior of the prediction error  $\hat{\mathcal{X}}_{n+1} - \mathcal{X}_{n+1}$  associated with the particular model/method used to perform the prediction. Thus, using some loss  $L(\hat{\mathcal{X}}_{n+1}, \mathcal{X}_{n+1})$  and based on the behavior of the corresponding bootstrap loss  $L(\hat{\mathcal{X}}_{n+1}^*, \mathcal{X}_{n+1}^*)$ , the proposed bootstrap procedure can also be applied to select between different predictors, the one which performs better. In the following, we demonstrate such an application of the bootstrap in selecting between the FAR(1) and the NFR method using the behavior of the bootstrap estimator of the (conditional) mean square error of prediction, i.e., of  $E^*[(\hat{\mathcal{X}}_{n+1}^*(\tau) - \mathcal{X}_{n+1}^*(\tau))^2 | \mathcal{X}_n]$ ,  $\tau \in [0, 1]$ .

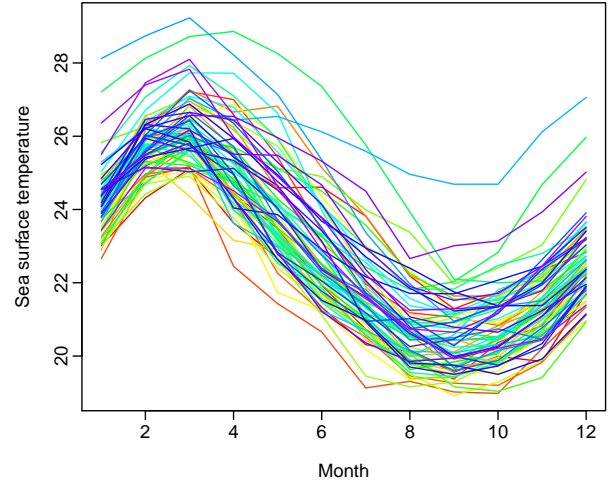
## 6.1 Monthly Sea Surface Temperature Data Set

Consider the monthly sea surface temperatures from January 1950 to December 2018 available at <https://www.cpc.ncep.noaa.gov/data/indices/ersst5.nino.mth.81-10.ascii>. These averaged sea surface temperatures were measured by moored buoys in the “Niño region”. We consider all four Niño regions: Niño 1+2 is defined by the coordinates 0 – 10° South, 90 – 80° West; Niño 3 is defined by the coordinates 5° North – 5° South, 150° – 90° West; Niño 4 is defined by the coordinates 5° North – 5° South, 160° East – 150° West; Niño 3+4 is defined by the coordinates 5° North – 5° South, 170 – 120° West. For the sea surface temperatures in Niño 1+2 region, univariate and functional time series plots are shown in Figure 2.

Applying the proposed bootstrap procedure and the two compared forecasting methods, we generate a set of  $B = 1,000$  bootstrap one-step-ahead prediction error curves  $\mathcal{X}_{n+1}^* - \hat{\mathcal{X}}_{n+1}^*$ . These



(a) Univariate time series plot



(b) Functional time series plot

Figure 2: Time series (left panel) and rainbow plots (right panel) of sea surface temperatures in Niño 1+2 region from January 1982 to December 2017.

are presented in the left panel of Figure 3 for the FAR(1) predictor and in the right panel of the same figure for the NFR predictor.

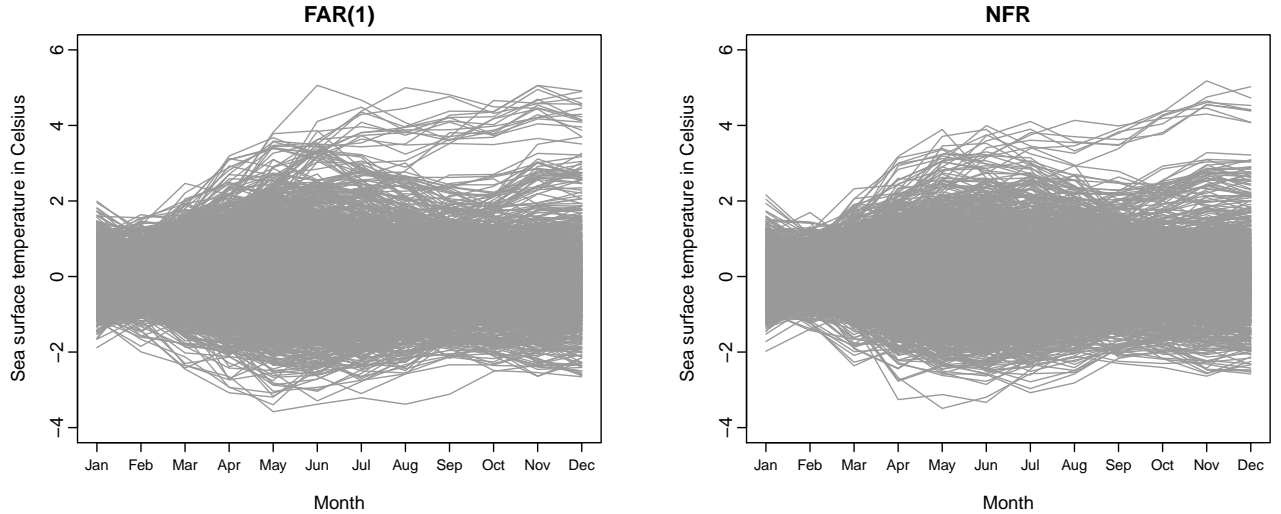


Figure 3: Bootstrap-generated one-step-ahead prediction error curves for the sea surface temperature data using the FAR(1) model (left panel) and the NFR method (right panel).

In Figure 4a, we present the bootstrap estimates of the (conditional) mean square error  $E[(\hat{\mathcal{X}}_{n+1}(\tau_j) - \mathcal{X}_{n+1}(\tau_j))^2 | \mathcal{X}_n]$ ,  $j = 1, 2, \dots, J$ , of the two prediction methods. As shown in this figure, the mean square error produced by the NFR method is uniformly (across all points  $\tau_1, \tau_2, \dots, \tau_J$ ) smaller than the corresponding mean square prediction error produced using the

FAR(1) method. Thus, for this functional time series, using the NFR method to perform the one-step-ahead prediction seems preferable. The point prediction using this method as well as the corresponding 80% and 95% simultaneous prediction bands are shown in Figure 4b.

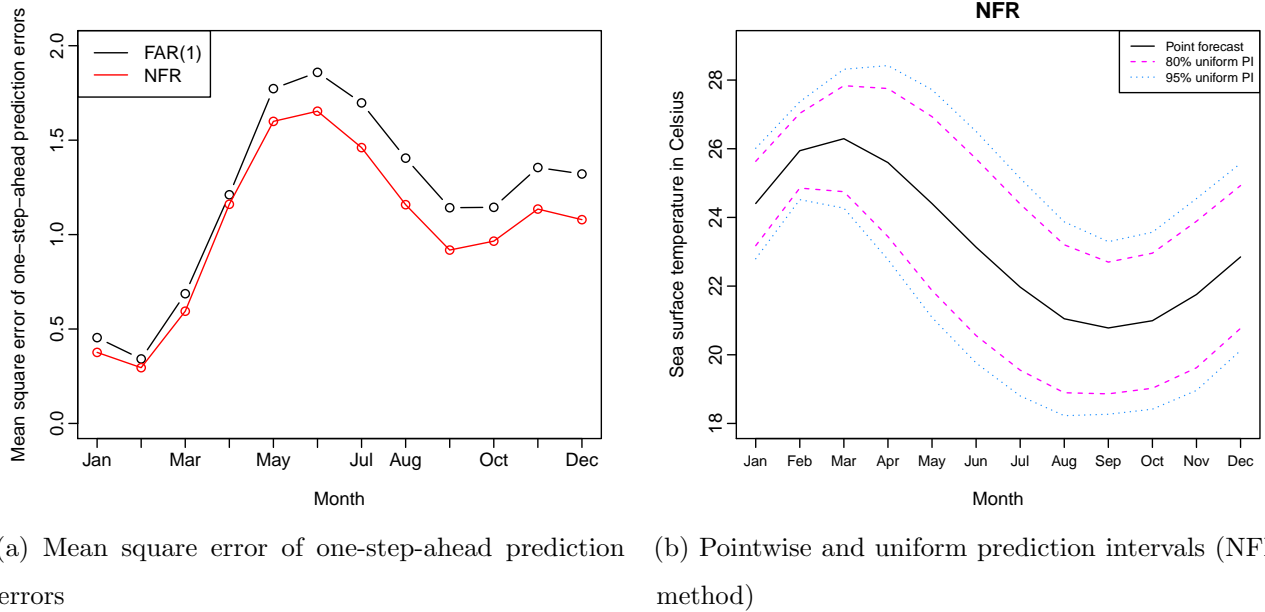


Figure 4: Bootstrap estimates of the mean square error of the one-step-ahead prediction for the FAR(1) model and the NFR method (left panel). Point forecast together with 80% and 95% simultaneous prediction bands using the NFR method (right panel).

## 7 Conclusions

We have presented a novel bootstrap method for the construction of prediction bands for a functional time series. In a model-free way, our method generates future functional pseudo-random elements that allow for valid estimation of the conditional distribution of the prediction error that a user-selected prediction method produces. The obtained bootstrap estimates of the prediction error distribution consider the innovation and the estimation errors associated with prediction and the error arising from a different model being used for prediction than the one generating the functional time series observed. Theoretical results were presented to justify using the proposed bootstrap method in constructing prediction bands that also appropriately consider the local variability of the conditional distribution of the prediction error. We have demonstrated the good finite sample performance of the bootstrap method presented through a series of simulations. The

real-life data sets analyzed have demonstrated the capabilities and the good finite sample behavior of the presented bootstrap method for the construction of prediction bands.

## SUPPLEMENTARY MATERIAL

This supplementary material contains the analysis of a second real data example, the derivation of Condition (16), some auxiliary lemmas and the proofs of the theoretical results presented in the main paper.

### 8 Intraday $\text{PM}_{10}$ Data Set

We analyze the half-hourly measurements of the concentration of particulate matter with an aerodynamic diameter of less than 10um in ambient air taken in Graz, Austria, from October 1, 2010, to March 31, 2011. We convert  $N = 8,736$  discrete univariate time series points into  $n = 182$  daily curves. A univariate time series display of intraday pollution curves is given in Figure 5a, with the same data shown in Figure 5b as a time series of functions.

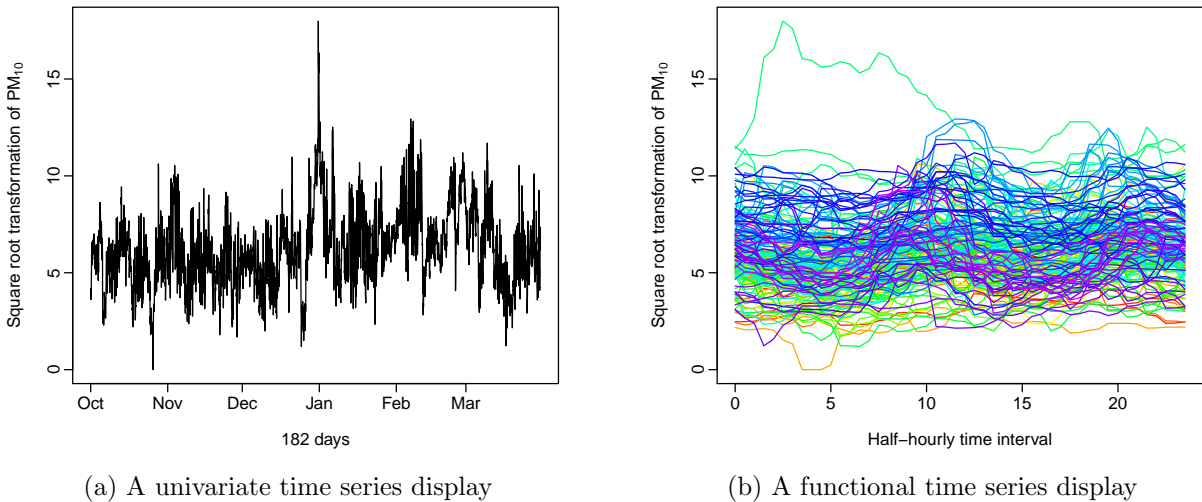


Figure 5: Graphical displays of intraday measurements of the  $\text{PM}_{10}$  from October 1, 2010, to March 31, 2011, in Graz, Austria.

Using the bootstrap procedure, we construct one- and two-step-ahead prediction bands for this functional time series. We first generate  $B = 1,000$  functional pseudo-time series, and we apply the FAR(1) and the NFR forecasting methods to obtain a set of one-step-ahead prediction error curves.

These are displayed in Figure 6. In the left panel of Figure 7, we show the bootstrap estimates of the (conditional) mean square prediction error  $E[(\hat{\mathcal{X}}_{n+1}(\tau_j) - \mathcal{X}_{n+1}(\tau_j))^2 | \mathcal{X}_n]$ ,  $j = 1, 2, \dots, J$ , obtained using the FAR(1) and NFR methods. As this figure shows, neither of the two methods is uniformly (i.e., across all points  $\tau_j \in [0, 1]$ ) better, with the FAR(1) method having a slight advantage. In particular, the bootstrap estimated conditional, root mean square error (RMSE) of the FAR(1) method is 1.451 compared with 2.054 of the NFR method.

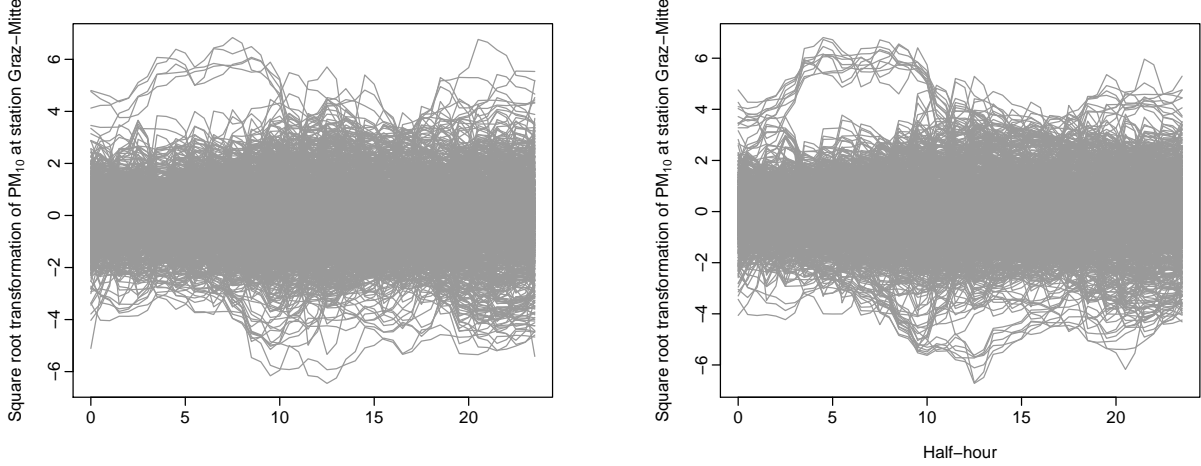


Figure 6: One-step-ahead prediction error curves for the intraday  $\text{PM}_{10}$  data using the FAR(1) model (left panel) and the NFR method (right panel).

We apply the FAR(1) method to perform the prediction for  $h = 1$  and  $h = 2$ . The corresponding bootstrap-based simultaneous prediction bands for  $h = 1$ , are displayed in the right panel of Figure 7.

In contrast to the relatively small sample size of  $n = 69$  curves of the Monthly Sea Surface Temperature data analyzed in the previous example, the sample size of  $n = 182$  curves of the intraday  $\text{PM}_{10}$  data considered in this section allows us to further evaluate the performance of the FAR(1) prediction method. For this, we use the observed data from October 1, 2010, to January 30, 2011, as the initial training sample, and we produce one- and two-step-ahead forecasts by increasing the training sample by one curve each time. We iterate this procedure until the training sample contains all the observed data. In this way, we construct 60 one-step and 59 two-step-ahead forecasts, enabling us to assess the interval forecast accuracy of the FAR(1) method. The results obtained for  $h = 1$  and  $h = 2$  are shown in Table 4. The FAR(1) prediction performs well for this functional time series, and the proposed bootstrap method produces for both forecasting steps, prediction intervals, the empirical coverages of which are close to the desired nominal levels. Notice that, as it is expected, the uncertainty associated with  $h = 2$  is larger than that for  $h = 1$ .

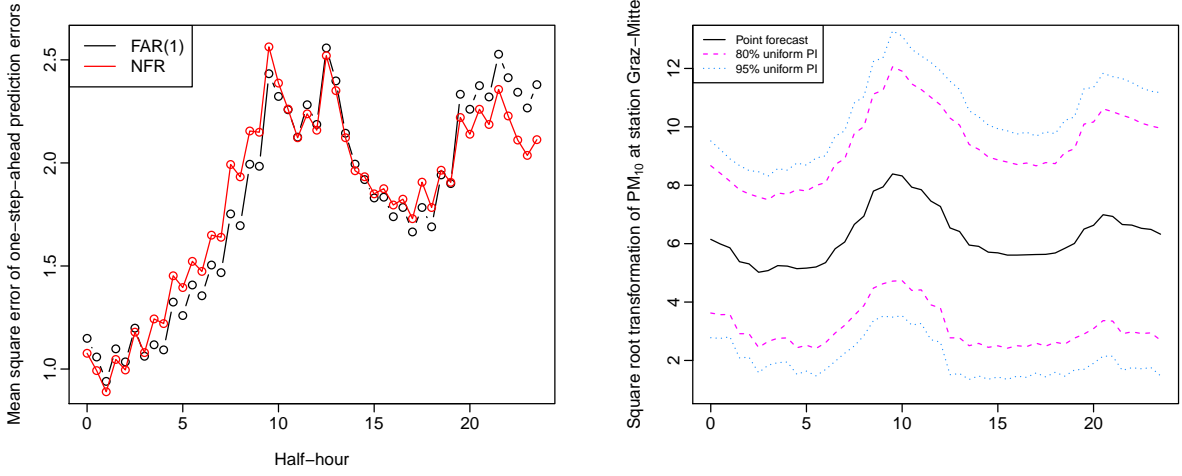


Figure 7: Bootstrap estimates of the mean square error of the one-step-ahead prediction for the FAR(1) model and the NFR method (left panel). Point forecast together with 80% and 95% simultaneous prediction bands using the FAR(1) method (right panel).

Table 4: Evaluation of the interval forecast accuracy at the forecast horizons  $h = 1$  and  $h = 2$  for the  $PM_{10}$  data set using the FAR(1) model for prediction and the sieve bootstrap procedure with 1000 bootstrap replications.

Nominal coverage	Criterion	$h = 1$	$h = 2$
80%	$CPD_{\text{pointwise}}$	0.789	0.777
	$\bar{S}_{\alpha=0.2}$	5.189	7.572
	$CPD_{\text{uniform}}$	0.833	0.777
95%	$CPD_{\text{pointwise}}$	0.943	0.923
	$\bar{S}_{\alpha=0.05}$	7.528	10.941
	$CPD_{\text{uniform}}$	0.917	0.901

## 9 Auxiliary Results and Proofs

Recall that  $\mathcal{X}_{n+h} = \sum_{j=1}^m \mathbf{1}_j^\top \boldsymbol{\xi}_{n+h} v_j + U_{n+h,m}$ ,  $\hat{\mathcal{X}}_{n+h} = \hat{g}_{(h)}(\mathcal{X}_n, \dots, \mathcal{X}_{n-k+1})$ ,  $\mathcal{X}_{n+h}^* = \sum_{j=1}^m \mathbf{1}_j^\top \boldsymbol{\xi}_{n+h}^* \hat{v}_j + U_{n+h,m}^*$  and  $\hat{\mathcal{X}}_{n+h}^* = \hat{g}_{(h)}^*(\mathcal{X}_n, \dots, \mathcal{X}_{n-k+1})$ . Define  $\mathcal{X}_{n+h,m}^+ = \sum_{j=1}^m \mathbf{1}_j^\top \boldsymbol{\xi}_{n+h}^+ v_j$ , where  $\boldsymbol{\xi}_{n+h}^+ = \sum_{j=1}^p \tilde{A}_{j,p} \boldsymbol{\xi}_{n+h-j} + \mathbf{e}_{n+h}^+$ , with  $\mathbf{e}_{n+h}^+$  i.i.d. resampled from the set  $\{\tilde{\mathbf{e}}_t - \tilde{\mathbf{e}}_n, t = p+1, p+2, \dots, n\}$ ,  $\tilde{\mathbf{e}}_n = (n-p)^{-1} \sum_{t=p+1}^n \tilde{\mathbf{e}}_t$ , and  $\tilde{\mathbf{e}}_t = \boldsymbol{\xi}_t - \sum_{j=1}^p \tilde{A}_{j,p} \boldsymbol{\xi}_{t-j}$ ,  $t = p+1, p+2, \dots, n$ ,

are the residuals obtained from an autoregressive fit based on the time series of true scores  $\xi_1, \xi_2, \dots, \xi_n$ .

**Derivation of Condition in (16):** Note that the assumption  $\lambda_j - \lambda_{j+1} \geq Cj^{-\vartheta}$  for  $j = 1, 2, \dots$ , implies that  $1/\lambda_j \leq C^{-1}j^\vartheta$ . For  $p = O(n^\gamma)$  and  $m = O(n^\delta)$ , with  $\gamma > 0$  and  $\delta > 0$ , Assumption 2(i) is satisfied if  $\delta < \gamma/4$ . Regarding Assumption 2(ii) verify that

$$\sqrt{\sum_{j=1}^m \frac{1}{\alpha_j^2}} \leq \frac{1}{C} \frac{1}{\sqrt{2\vartheta+1}} (m+1)^{\vartheta+1/2} = O(n^{\delta(\vartheta+1/2)}),$$

From this we get that

$$\frac{p^3}{\sqrt{nm}\lambda_m^2} \sqrt{\sum_{j=1}^m \frac{1}{\alpha_j^2}} = O(n^{3\gamma-1/2+3\vartheta\delta}).$$

i.e., Assumption 2(iii) is satisfied if  $\delta \leq (1-6\gamma)/(6\vartheta)$  and  $\gamma < 1/6$ . For Assumption 2(iii) and in the case of Yule Walker estimators, we have

$$\frac{m^6 p^4}{\lambda_m^2 \sqrt{n}} = O(n^{6\delta+4\gamma+2\vartheta\delta-1/2}),$$

which is fulfilled for  $\delta \leq (1-8\gamma)/(12+4\vartheta)$  and  $\gamma < 1/8$ . Note that for  $\gamma < 1/8$  and  $\delta > 0$ , the condition  $p^2/m^2 = O(\sqrt{n})$  also holds true. Putting the derived requirements on  $\gamma$  and  $\delta$  together, leads to condition in (15).  $\square$

**Lemma 9.1** *Let  $\Gamma_m(0) = E(\boldsymbol{\xi}_{n+h}\boldsymbol{\xi}_{n+h}^\top)$ ,  $\Gamma_m^+(0) = E(\boldsymbol{\xi}_{n+h}^+\boldsymbol{\xi}_{n+h}^{+\top})$  and  $\Gamma_m^*(0) = E(\boldsymbol{\xi}_{n+h}^*\boldsymbol{\xi}_{n+h}^{*\top})$ . If Assumption 1 and 2 are satisfied, then,*

$$\|\Gamma_m^+(0) - \Gamma_m(0)\|_F = O_P\left(\frac{m^2}{\sqrt{p}}\right).$$

*If Assumption 1 and 2' are satisfied, then*

$$\|\Gamma_m^*(0) - \Gamma_m(0)\|_F = O_P\left(\frac{p^5 \sqrt{m}}{\sqrt{n} \lambda_m^2} \sqrt{\sum_{j=1}^m \alpha_j^{-2}}\right).$$

**Proof:** Let  $\Psi_{j,p}$ ,  $\tilde{\Psi}_{j,p}$  and  $\hat{\Psi}_{j,p}$ ,  $j = 1, 2, \dots$ , be the coefficient matrices in the power series expansions of the inverse matrix polynomial  $(I_m - \sum_{j=1}^p A_{j,p} z^j)^{-1}$ ,  $(I_m - \sum_{j=1}^p \tilde{A}_{j,p} z^j)^{-1}$  and  $(I_m - \sum_{j=1}^p \hat{A}_{j,p} z^j)^{-1}$ , respectively,  $|z| \leq 1$ , where  $I_m$  is the  $m \times m$  unit matrix. Set  $\Psi_{0,p} = \tilde{\Psi}_{0,p} = \hat{\Psi}_{0,p} = I_m$  and let  $\Sigma_e = E(\mathbf{e}_{t,p} \mathbf{e}_{t,p}^\top)$ ,  $\tilde{\Sigma}_e = E(\tilde{\mathbf{e}}_{t,p} \tilde{\mathbf{e}}_{t,p}^\top)$  and  $\hat{\Sigma}_e = E(\hat{\mathbf{e}}_{t,p} \hat{\mathbf{e}}_{t,p}^\top)$ . Since

$$\Gamma_m(0) = \sum_{j=0}^{\infty} \Psi_{j,p} \Sigma_e \Psi_{j,p}^\top, \quad \Gamma_m^+(0) = \sum_{j=0}^{\infty} \tilde{\Psi}_{j,p} \tilde{\Sigma}_e \tilde{\Psi}_{j,p}^\top \quad \text{and} \quad \Gamma_m^*(0) = \sum_{j=0}^{\infty} \hat{\Psi}_{j,p} \hat{\Sigma}_e \hat{\Psi}_{j,p}^\top,$$

the assertion of the lemma follows using the same arguments as in the proof of Lemma 6.5 of Paparoditis (2018) and the bounds

$$\sum_{j=1}^{\infty} \|\tilde{\Psi}_{j,p} - \Psi_{j,p}\|_F = o_P\left(m^{3/2}/\sqrt{p}\right) \quad \text{and} \quad \sum_{j=1}^{\infty} \|\hat{\Psi}_{j,p} - \tilde{\Psi}_{j,p}\|_F = O_P\left(\frac{p^5\sqrt{m}}{\sqrt{n}\lambda_m^2} \sqrt{\sum_{j=1}^m \alpha_j^{-2}}\right),$$

obtained in the aforementioned paper.  $\square$

**Lemma 9.2** *Let  $\hat{g}, g : \mathcal{H}^k \rightarrow \mathcal{H}$ . For  $x = (x_1, x_2, \dots, x_k) \in \mathcal{H}^k$  and  $h \in \mathbb{N}$ , let*

$$\hat{g}_{(h)}(x) = \hat{g}(\hat{g}_{(h-1)}(x), \hat{g}_{(h-2)}(x), \dots, (\hat{g}_{(h-k)}(x))),$$

where  $\hat{g}_{(1)}(x) = \hat{g}(x)$  and  $\hat{g}_{(s)}(x) = x_{1-s}$  if  $s \leq 0$ . Define analogously  $g_{(h)}(x)$ . If  $\|\hat{g} - g_0\|_{\mathcal{L}} \xrightarrow{P} 0$  then,  $\|\hat{g}_{(h)}(x) - g_{0,(h)}(x)\|_2 \xrightarrow{P} 0$  for any  $h \in \mathbb{N}$ .

**Proof:** We use the notation  $y_n = (\hat{g}_{(L)}(x), \dots, \hat{g}_{(L-k+1)}(x))$  and  $y = (g_{0,(L)}(x), \dots, g_{0,(L-k+1)}(x))$ .

For  $h = 1$  we have

$$\|\hat{g}(x) - g_0(x)\|_2 \leq \|\hat{g} - g_0\|_{\mathcal{L}} \|x\|_2 = o_P(1)O(1) = o_P(1),$$

since  $\|\hat{g} - g_0\|_{\mathcal{L}} \xrightarrow{P} 0$ . Suppose that  $\|\hat{g}_{(L)}(x) - g_{0,(L)}(x)\|_2 \xrightarrow{P} 0$  for some  $L \in \mathbb{N}$ . Then,

$$\begin{aligned} \|\hat{g}_{(L+1)}(x) - g_{0,(L+1)}(x)\|_2 &\leq \|\hat{g}(y_n) - g_0(y_n)\|_2 \\ &\quad + \|g_0(y_n) - g_0(y)\|_2 \\ &\leq \|\hat{g} - g_0\|_{\mathcal{L}} \|y_n\|_2 + \|g_0\|_{\mathcal{L}} \sum_{l=0}^{k-1} \|\hat{g}_{(L-l)}(x) - g_{0,(L-l)}(x)\|_2 \\ &= o_P(1)O_P(1) + O(1)o_P(1) = o_P(1). \end{aligned}$$

$\square$

**Proof of Proposition 3.1:** We first show that under the conditions of the proposition, and for every  $h \in \mathbb{N}$  the following is true,

$$\sup_{\tau \in [0,1]} E \int_0^1 (\tilde{c}_{g,h}(\tau, s) - c_{g,h}(\tau, s))^2 ds \rightarrow 0, \quad (24)$$

where  $c_{g,h}$  and  $\tilde{c}_{g,h}$  are the kernels associated with the operators  $g_{(h)}$  and  $\tilde{g}_{(h)}$  respectively. These kernels satisfy  $c_{g,h}(\tau, s) = \int_0^1 c_{g,h-1}(\tau, u) c_{g,1}(u, s) du$  with  $c_{g,1}(\tau, s) = c_g(\tau, s)$  and  $\tilde{c}_{g,h}$  defined similarly. Notice that for  $h = 1$ , assertion (24) is true by assumption. Suppose that the assertion is true for some  $h \in \mathbb{N}$ . Using  $(a + b)^2 \leq 2a^2 + 2b^2$  as well as Cauchy-Schwarz's inequality, we get

$$\begin{aligned} \int_0^1 (\tilde{c}_{g,h+1}(\tau, s) - c_{g,h+1}(\tau, s))^2 ds &\leq 2 \int_0^1 (\tilde{c}_{g,h}(\tau, u) - c_{g,h}(\tau, u))^2 du \int_0^1 \int_0^1 \tilde{c}_g^2(u, s) dud s \\ &\quad + 2 \int_0^1 c_{g,h}^2(\tau, u) du \int_0^1 \int_0^1 (\tilde{c}_g(u, s) - c_g(u, s))^2 dud s. \end{aligned}$$

From this we have

$$\begin{aligned}
\sup_{\tau \in [0,1]} E \int_0^1 (\tilde{c}_{g,h+1}(\tau, s) - c_{g,h+1}(\tau, s))^2 ds &\leq 2 \sup_{\tau \in [0,1]} E \int_0^1 (\tilde{c}_{g,h}(\tau, u) - c_{g,h}(\tau, u))^2 du \|\tilde{g}\|_{HS}^2 \\
&\quad + 2 \sup_{\tau \in [0,1]} \int_0^1 c_{g,h}^2(\tau, u) du E \|\tilde{g} - g\|_{HS}^2 \\
&\leq C \left\{ \sup_{\tau \in [0,1]} E \int_0^1 (\tilde{c}_{g,h}(\tau, u) - c_{g,h}(\tau, u))^2 du + E \|\tilde{g} - g\|_{HS}^2 \right\} \rightarrow 0.
\end{aligned}$$

Using (24) we prove by induction that Assumption 3' is satisfied. For  $h = 1$  we have

$$\sup_{\tau \in [0,1]} E |\tilde{g}(x)(\tau) - g(x)(\tau)|^2 \leq \|x\|_2^2 \sup_{\tau \in [0,1]} E \int_0^1 (\tilde{c}_g(\tau, s) - c_g(\tau, s))^2 ds \rightarrow 0.$$

Suppose that the assertion is true for some  $h \in \mathbb{N}$ . Using Cauchy-Schwarz's inequality and the bound  $\|g(x)\| \leq \|g\|_{HS} \|x\|$ , we get for  $h + 1$ ,

$$\begin{aligned}
\sup_{\tau \in [0,1]} E |\tilde{g}_{(h+1)}(x)(\tau) - g_{(h+1)}(x)(\tau)|^2 &\leq 2 \sup_{\tau \in [0,1]} E \left| \int_0^1 (\tilde{c}_{g,h}(\tau, s) - c_{g,h}(\tau, s)) \tilde{g}(x)(s) ds \right|^2 \\
&\quad + 2 \sup_{\tau \in [0,1]} E \left| \int_0^1 c_{g,h}(\tau, s) (\tilde{g}(x) - g(x))(s) ds \right|^2 \\
&\leq 2 \sup_{\tau \in [0,1]} E \int_0^1 (\tilde{c}_{g,h}(\tau, s) - c_{g,h}(\tau, s))^2 ds \int_0^1 \tilde{g}^2(x)(s) ds \\
&\quad + 2 \sup_{\tau \in [0,1]} \int_0^1 c_{g,h}^2(\tau, s) E \int_0^1 (\tilde{g}(x) - g(x))^2(s) ds \\
&\leq 2 \|x\|_2^2 \sup_{\tau \in [0,1]} E \int_0^1 (\tilde{c}_{g,h}(\tau, s) - c_{g,h}(\tau, s))^2 ds \|\tilde{g}\|_{HS}^2 \\
&\quad + 2 \|x\|_2^2 \sup_{\tau \in [0,1]} \int_0^1 c_{g,h}^2(\tau, s) E \|\tilde{g} - g\|_{HS}^2 \rightarrow 0.
\end{aligned}$$

□

**Proof of Theorem 3.1:** Recall the notation  $\mathcal{X}_{n,k} = (\mathcal{X}_{n-k+1}, \mathcal{X}_{n-k+2}, \dots, \mathcal{X}_n)$ . Observe that

$$\begin{aligned}
\|\widehat{g}_{(h)}(\mathcal{X}_{n,k}) - \widehat{g}_{(h)}^*(\mathcal{X}_{n,k})\|_2 &\leq \|\widehat{g}_{(h)}(\mathcal{X}_{n,k}) - g_{0,(h)}(\mathcal{X}_{n,k})\|_2 + \|\widehat{g}_{(h)}^*(\mathcal{X}_{n,k}) - g_{0,(h)}(\mathcal{X}_{n,k})\|_2 \\
&= o_P(1),
\end{aligned}$$

where the last equality follows by Assumption 3, Lemma 9.2 and the fact that  $\|\mathcal{X}_{n,k}\|_2 = O_P(1)$ .

Hence  $\mathcal{E}_{n+h} - \mathcal{E}_{n+h}^* = \sum_{j=1}^{\infty} \mathbf{1}_j^\top \boldsymbol{\xi}_{n+h} v_j - \left( \sum_{j=1}^m \mathbf{1}_j^\top \boldsymbol{\xi}_{n+h}^* \widehat{v}_j + U_{n+h,m}^* \right) + o_P(1)$  and by Slutsky's theorem, it suffices to show that

$$d\left( \sum_{j=1}^{\infty} \mathbf{1}_j^\top \boldsymbol{\xi}_{n+h} v_j, \sum_{j=1}^m \mathbf{1}_j^\top \boldsymbol{\xi}_{n+h}^* \widehat{v}_j + U_{n+h,m}^* \right) = o_P(1). \quad (25)$$

Assertion (25) follows if we show that,

- (i)  $d(\sum_{j=1}^m \xi_{j,n+h}^+ v_j, \sum_{j=1}^\infty \xi_{j,n+h} v_j) \rightarrow 0$ ,
- (ii)  $\|\sum_{j=1}^m \mathbf{1}_j^\top \boldsymbol{\xi}_{n+h}^* \widehat{v}_j - \sum_{j=1}^m \mathbf{1}_j^\top \boldsymbol{\xi}_{n+h}^+ v_j\|_2 \xrightarrow{P} 0$ , and,
- (iii)  $U_{n+h,m}^* \xrightarrow{P} 0$ .

To establish (i) consider the sequence  $\{Y_n^+(h)\}$  in  $\mathcal{H}$ , where  $Y_n^+(h) = \sum_{j=1}^\infty \widetilde{\xi}_{j,n+h} v_j$  and  $\widetilde{\xi}_{j,n+h} = \xi_{j,n+h}^+$  for  $j = 1, 2, \dots, m$  and  $\widetilde{\xi}_{j,n+h} = 0$  for  $j \geq m+1$ . For  $k \in \mathbb{N}$ , let  $Y_{n,k}^+(h) = \sum_{j=1}^k \widetilde{\xi}_{j,n+h} v_j$ . By Theorem 3.2 of Billingsley (1999), assertion (i) follows if we show that

- (a)  $Y_{n,k}^+(h) \xrightarrow{d} Y_k(h) = \sum_{j=1}^k \xi_{j,n+h} v_j$  for any  $k \in \mathbb{N}$ , as  $n \rightarrow \infty$ .
- (b)  $Y_k(h) \xrightarrow{d} Y(h) = \sum_{j=1}^\infty \xi_{j,n+h} v_j$ , as  $k \rightarrow \infty$ .
- (c) For any  $\epsilon > 0$ ,  $\lim_{k \rightarrow \infty} \limsup_{n \in \mathbb{N}} P(\|Y_{n,m}^+(h) - Y_{n,k}^+(h)\|_2 > \epsilon) = 0$ .

Consider (a). Assume that  $n$  is large enough such that  $m > k$ . Since  $k$  is fixed,  $(\widetilde{\xi}_{1,n+h}, \widetilde{\xi}_{2,n+h}, \dots, \widetilde{\xi}_{k,n+h})^\top = (\xi_{1,n+h}^+, \xi_{2,n+h}^+, \dots, \xi_{k,n+h}^+)^\top = \boldsymbol{\xi}_{n+h}^+(k)$  where the latter vector is obtained as  $\boldsymbol{\xi}_{n+h}^+(k) = I_{k,m} \boldsymbol{\xi}_{n+h}^+$  with  $I_{k,m}$  the  $k \times m$  matrix with elements  $(j, j)$ ,  $j = 1, 2, \dots, k$ , equal to one and zero else. Assume that  $h = 1$ . Then, the vector  $\boldsymbol{\xi}_{n+1}^+$  is generated via the regression type autoregression  $\boldsymbol{\xi}_{n+1}^+ = \sum_{j=1}^p \widetilde{A}_{j,p} \boldsymbol{\xi}_{n+1-j}^+ + e_{n+1}^+$  and  $e_{n+1}^+$  i.i.d. innovations. Therefore, and since  $k$  is fixed, we have by standard arguments (see Lemma 3.1 of Meyer & Kreiss (2015)), that  $\boldsymbol{\xi}_{n+1}^+(k) \xrightarrow{d} \boldsymbol{\xi}_{n+1}(k) = (\xi_{1,n+1}, \xi_{2,n+1}, \dots, \xi_{k,n+1})^\top$ . Suppose that the assertion is true for some  $h \in \mathbb{N}$ . For  $h+1$  it follows by similar arguments and using the recursion  $\boldsymbol{\xi}_{n+h+1}^+ = \sum_{j=1}^p \widetilde{A}_{j,p} \boldsymbol{\xi}_{n+h+1-j}^+ + e_{n+h+1}^+$  that  $\boldsymbol{\xi}_{n+h+1}^+(k) \xrightarrow{d} \boldsymbol{\xi}_{n+h+1}(k) = (\xi_{1,n+h+1}, \xi_{2,n+h+1}, \dots, \xi_{k,n+h+1})^\top$ . By the continuous mapping theorem we then conclude that  $Y_{n,k}^+(h) \xrightarrow{d} \sum_{j=1}^k \xi_{j,n+h} v_j = Y_{n,k}(h)$ . Consider (b). Notice that,  $E\|Y_k^+(h) - Y(h)\|_2^2 = E\|\sum_{j=k+1}^\infty \xi_{j,n+h} v_j\|_2^2 = \sum_{j=k+1}^\infty \lambda_j \rightarrow 0$ , as  $k \rightarrow \infty$ , which by Markov's inequality and Slutsky's theorem implies that  $Y_k(h) \xrightarrow{d} \sum_{j=1}^\infty \xi_{j,n+h} v_j$  as  $k \rightarrow \infty$ . Consider (c). We have

$$\begin{aligned} E\|Y_{n,m}(h) - Y_{n,k}^+(h)\|_2^2 &= E\left\|\sum_{j=k+1}^m \xi_{j,n+h}^+ v_j\right\|_2^2 \\ &= \sum_{j=k+1}^m \mathbf{1}_j^\top \Gamma_m^+(0) \mathbf{1}_j = \sum_{j=k+1}^m \lambda_j + \sum_{j=k+1}^m \mathbf{1}_j^\top (\Gamma_m^+(0) - \Gamma_m(0)) \mathbf{1}_j. \end{aligned}$$

Now since  $|\sum_{j=k+1}^m \mathbf{1}_j^\top (\Gamma_m^+(0) - \Gamma_m(0)) \mathbf{1}_j| = O_P(\sqrt{m} \|\Gamma_m^+(0) - \Gamma_m(0)\|_F)$ , we get by Lemma 9.1, Assumption 2 and Markov's inequality that

$$\limsup_{n \in \mathbb{N}} P(\|Y_{n,m}^+(h) - Y_{n,k}^+(h)\|_2 > \epsilon) \leq \frac{1}{\epsilon^2} \left\{ \sum_{j=k+1}^\infty \lambda_j + O_P(\sqrt{m} \|\Gamma_m^+(0) - \Gamma_m(0)\|_F) \right\},$$

which converges to zero as  $k \rightarrow \infty$ .

Consider assertion (ii). Since  $\|\widehat{v}_j\|_2 = 1$ , we get the bound

$$\begin{aligned}
\left\| \sum_{j=1}^m \mathbf{1}_j^\top (\boldsymbol{\xi}_{n+h}^+ v_j - \boldsymbol{\xi}_{n+h}^* \widehat{v}_j) \right\|_2 &\leq \left\| \sum_{j=1}^m \mathbf{1}_j^\top (\boldsymbol{\xi}_{n+h}^+ - \boldsymbol{\xi}_{n+h}^*) \widehat{v}_j \right\|_2 \\
&\quad + \left\| \sum_{j=1}^m \mathbf{1}_j^\top \boldsymbol{\xi}_{n+h}^+ (\widehat{v}_j - v_j) \right\|_2 \\
&\leq \sqrt{m} \|\boldsymbol{\xi}_{n+h}^* - \boldsymbol{\xi}_{n+h}^+\|_2 + \|\boldsymbol{\xi}_{n+h}^+\|_2 \sum_{j=1}^m \|\widehat{v}_j - v_j\|_2 \\
&= \sqrt{m} \|\boldsymbol{\xi}_{n+h}^* - \boldsymbol{\xi}_{n+h}^+\|_2 + O_P\left(\frac{m}{\sqrt{n}} \sqrt{\sum_{j=1}^m \alpha_j^{-2}}\right),
\end{aligned}$$

where the last equality follows using  $\|\boldsymbol{\xi}_{n+h}^+\|_2^2 = O_P(m)$  and Lemma 3.2 of [Hörmann & Kokoszka \(2010\)](#). To evaluate the first term on the right hand side of the last displayed inequality, we use the bound

$$\begin{aligned}
\|\boldsymbol{\xi}_{n+h}^* - \boldsymbol{\xi}_{n+h}^+\|_2 &\leq \left\| \sum_{j=1}^p (\widehat{A}_{j,p} - \widetilde{A}_{j,p}) \boldsymbol{\xi}_{n+h-j}^* \right\|_2 + \left\| \sum_{j=1}^p \widetilde{A}_{j,p} (\boldsymbol{\xi}_{n+h-j}^+ - \boldsymbol{\xi}_{n+h-j}^*) \right\|_2 + \|\mathbf{e}_{n+h}^* - \mathbf{e}_{n+h}^+\|_2 \\
&= \sum_{j=1}^3 T_{j,n},
\end{aligned} \tag{26}$$

with an obvious notation for  $T_{j,n}$ ,  $j = 1, 2, 3$ . Observe first that  $E\|\mathbf{e}_{n+h}^* - \mathbf{e}_{n+h}^+\|_2^2 \rightarrow 0$  in probability, as in the proof of Lemma 6.7 in [Paparoditis \(2018\)](#), that is  $T_{3,n} \xrightarrow{P} 0$ . For the first term of (26) we have

$$\begin{aligned}
T_{1,n} &= \left\| \sum_{j=1}^p (\widehat{A}_{j,p} - \widetilde{A}_{j,p}) \boldsymbol{\xi}_{n+h-j}^* \right\|_2 \leq \sum_{j=1}^p \|\widehat{A}_{j,p} - \widetilde{A}_{j,p}\|_F \|\boldsymbol{\xi}_{n+h-j}^*\|_2 \\
&= O_P(\sqrt{mp} \|\widehat{A}_{p,m} - \widetilde{A}_{p,m}\|_F) = O_P\left(\frac{m^{3/2} p^{5/2}}{\lambda_m^2} \sqrt{\frac{1}{n} \sum_{j=1}^m \alpha_j^{-2}}\right) \rightarrow 0,
\end{aligned}$$

because  $\|\widehat{A}_{p,m} - \widetilde{A}_{p,m}\|_F = O_P((p\sqrt{m}\lambda_m^{-1} + p^2)^2 \sqrt{n^{-1} \sum_{j=1}^m \alpha_j^{-2}})$ , see [Paparoditis \(2018, p. 5 of the Supplementary Material\)](#), and the last equality follows by Assumption 2. To show that  $T_{2,n} \xrightarrow{P} 0$ , we first show that, for any  $h \in \mathbb{N}$ ,

$$\sum_{j=1}^p \|\boldsymbol{\xi}_{n+h-j}^+ - \boldsymbol{\xi}_{n+h-j}^*\|_2^2 \xrightarrow{P} 0, \tag{27}$$

For  $h = 1$  we have

$$\begin{aligned}
\sum_{j=1}^p \|\xi_{n+h-j}^+ - \xi_{n+h-j}^*\|_2^2 &= \sum_{j=1}^p \|\xi_{n+h-j} - \widehat{\xi}_{n+h-j}\|_2^2 \\
&\leq \sum_{j=1}^p \|\mathcal{X}_{n+h-j}\|_2^2 \sum_{j=1}^m \|\widehat{v}_j - v_j\|_2^2 \\
&= O_P\left(p \sum_{j=1}^m \|\widehat{v}_j - v_j\|_2^2\right) = O_P\left(\frac{p}{n} \sum_{j=1}^m \alpha_j^{-2}\right) \rightarrow 0.
\end{aligned}$$

Assume that the assertion is true for some  $h \in \mathbb{N}$ . We then have for  $h + 1$  that

$$\begin{aligned}
\sum_{j=1}^p \|\xi_{n+h+1-j}^+ - \xi_{n+h+1-j}^*\|_2^2 &= \|\xi_{n+h}^+ - \xi_{n+h}^*\|_2^2 + o_P(1) \\
&\leq 4 \left\| \sum_{j=1}^p (\widehat{A}_{j,p} - \widetilde{A}_{j,p}) \xi_{n+h-j}^* \right\|_2^2 + 4 \left\| \sum_{j=1}^p \widetilde{A}_{j,p} (\xi_{n+h-j}^+ - \xi_{n+h-j}^*) \right\|_2^2 \\
&\quad + 2 \|\mathbf{e}_{h+h}^+ - \mathbf{e}_{n+h}^*\|_2^2 + o_P(1),
\end{aligned}$$

which converges to zero in probability by the same arguments as those used in the proof that  $T_{1,n}$  and  $T_{3,n}$  converge to zero in probability and because

$$\left\| \sum_{j=1}^p \widetilde{A}_{j,p} (\xi_{n+h-j}^+ - \xi_{n+h-j}^*) \right\|_2^2 \leq \sum_{j=1}^p \|\widetilde{A}_{j,p}\|_F^2 \sum_{j=1}^p \|\xi_{n+h-j}^+ - \xi_{n+h-j}^*\|_2^2 = O_P(1) \cdot o_P(1),$$

using the fact that  $\sum_{j=1}^p \|\widetilde{A}_{j,p}\|_F^2 = O_P(1)$  uniformly in  $m$  and  $p$ ; see the proof of Lemma 6.5 in [Paparoditis \(2018\)](#). Using (27), we get for the term  $T_{2,n}$ ,

$$T_{2,n}^2 = \left\| \sum_{j=1}^p \widetilde{A}_{j,p} (\xi_{n+h-j}^+ - \xi_{n+h-j}^*) \right\|_2^2 \leq \sum_{j=1}^p \|\widetilde{A}_{j,p}\|_F^2 \sum_{j=1}^p \|\xi_{n+h-j}^+ - \xi_{n+h-j}^*\|_2^2 = O_P(1) \cdot o_P(1) \rightarrow 0.$$

It remains to prove assertion (iii). This follows from Markov's inequality and the fact that  $E^* \|U_{n+h,m}^*\|_2^2 \rightarrow 0$  in probability. The last statement is true since

$$\begin{aligned}
E^* \|U_{n+h,m}^*\|_2^2 &= \frac{1}{n} \sum_{t=1}^n \|\widehat{U}_{t,m} - \overline{U}_n\|_2^2 \\
&\leq \frac{4}{n} \sum_{t=1}^n \|\widehat{U}_{t,m} - U_{t,m}\|_2^2 + \frac{4}{n} \sum_{t=1}^n \|U_{t,m}\|_2^2 + 2 \|\overline{U}_n\|_2^2 \\
&= \frac{4}{n} \sum_{t=1}^n \left\| \sum_{j=1}^m \mathbf{1}_j^\top (\xi_t v_j - \widehat{\xi}_t \widehat{v}_j) \right\|_2^2 + o_P(1)
\end{aligned}$$

where the  $o_P(1)$  is due to the weak law of large numbers, the fact that  $E \|U_{t,m}\|^2 = \sum_{j=m+1}^\infty \lambda_j \rightarrow 0$  as  $m \rightarrow \infty$  and  $\overline{U}_{n,m} \rightarrow 0$ , in probability. For the first term on the right hand side of the last

displayed equality we have that this term is bounded by

$$\begin{aligned} & \frac{8}{n} \sum_{t=1}^n \left\| \sum_{j=1}^m \mathbf{1}_j^\top (\hat{\boldsymbol{\xi}}_t - \boldsymbol{\xi}_t) \hat{v}_j \right\|_2^2 + \frac{8}{n} \sum_{t=1}^n \left\| \sum_{j=1}^m \mathbf{1}_j^\top \boldsymbol{\xi}_t (\hat{v}_j - v_j) \right\|_2^2 \\ & \leq \frac{8}{n} \sum_{t=1}^n \|\mathcal{X}_t\|_2^2 \sum_{j=1}^m \|\hat{v}_j - v_j\|_2^2 + 8 \sqrt{\sum_{j,l=1}^m \left| \frac{1}{n} \sum_{t=1}^n \xi_{j,t} \xi_{l,t} \right|_2^2} \sum_{j=1}^m \|\hat{v}_j - v_j\|_2^2 = O_P(n^{-1} \sum_{j=1}^m \alpha_j^{-2}) \rightarrow 0, \end{aligned}$$

where the last equality follows because  $n^{-1} \sum_{t=1}^n \|\mathcal{X}_t\|_2^2 = O_P(1)$  and  $n^{-1} \sum_{t=1}^n \xi_{j,t} \xi_{l,t} \xrightarrow{P} \lambda_j \mathbf{1}_{j=l}$  as  $n \rightarrow \infty$ .  $\square$

**Proof of Theorem 3.2:** We only give the proof of assertion (20). We have

$$\begin{aligned} |\sigma_{n+h}^{*2}(\tau) - \sigma_{n+h}^2(\tau)| & \leq |E^*(\mathcal{X}_{n+h}^*(\tau))^2 - E(\mathcal{X}_{n+h}(\tau))^2| \\ & \quad + 2|EX_{n+h}(\tau)(\hat{g}_{(h)}(\mathcal{X}_{n,k})(\tau) - g_{0,(h)}(\mathcal{X}_{n,k})(\tau))| \\ & \quad + 2|E^*X_{n+h}^*(\tau)(\hat{g}_{(h)}^*(\mathcal{X}_{n,k})(\tau) - g_{0,(h)}(\mathcal{X}_{n,k})(\tau))| \\ & \quad + |E^*(\hat{g}_{(h)}^*(\mathcal{X}_{n,k})(\tau))^2 - g_{0,(h)}^2(\mathcal{X}_{n,k})(\tau)| + |E(\hat{g}_{(h)}(\mathcal{X}_{n,k})(\tau))^2 - g_{0,(h)}^2(\mathcal{X}_{n,k})(\tau)| \quad (28) \end{aligned}$$

Notice first that  $\sup_{\tau \in [0,1]} E^*(X_{n+h}^*(\tau))^2 = O_P(1)$  by equation (29) below and the fact that  $\sup_{\tau \in [0,1]} E(X_{n+h}(\tau))^2 = \sup_{\tau \in [0,1]} c(\tau, \tau) < \infty$ , by the continuity of the kernel  $c$ . Using Cauchy-Schwarz's inequality, and Assumption 3' we get,

$$\begin{aligned} & \sup_{\tau \in [0,1]} |EX_{n+h}(\tau)(\hat{g}_{(h)}(\mathcal{X}_{n,k})(\tau) - g_{0,(h)}(\mathcal{X}_{n,k})(\tau))| \\ & \leq \sup_{\tau \in [0,1]} E(X_{n+h}(\tau))^2 \sqrt{\sup_{\tau \in [0,1]} E(\hat{g}_{(h)}(\mathcal{X}_{n,k})(\tau) - g_{0,(h)}(\mathcal{X}_{n,k})(\tau))^2} \rightarrow 0, \\ & \sup_{\tau \in [0,1]} |E^*X_{n+h}^*(\tau)(\hat{g}_{(h)}^*(\mathcal{X}_{n,k})(\tau) - g_{0,(h)}(\mathcal{X}_{n,k})(\tau))| \\ & \leq \sup_{\tau \in [0,1]} E^*(X_{n+h}^*(\tau))^2 \sqrt{\sup_{\tau \in [0,1]} E^*(\hat{g}_{(h)}^*(\mathcal{X}_{n,k})(\tau) - g_{0,(h)}(\mathcal{X}_{n,k})(\tau))^2} \rightarrow 0. \end{aligned}$$

Using  $a^2 - b^2 = (a - b)(a + b)$ , Cauchy-Schwarz's inequality and Assumption 3' again, we get for the last two terms on the right hand side of the bound (28), that they also converges uniformly to zero, in probability. To establish assertion (20) it remains to show that

$$\sup_{\tau \in [0,1]} |E^*(\mathcal{X}_{n+h}^*(\tau))^2 - E(\mathcal{X}_{n+h}(\tau))^2| \rightarrow 0, \quad (29)$$

in probability. Notice first that due to the independence of  $\sum_{j=1}^m \mathbf{1}_j^\top \boldsymbol{\xi}_{n+h}^* \hat{v}_j$  and  $U_{n+h,m}^*$  we have  $E^*(\mathcal{X}_{n+h}^*(\tau))^2 = E^*(\sum_{j=1}^m \mathbf{1}_j^\top \boldsymbol{\xi}_{n+h}^* \hat{v}_j(\tau))^2 + E^*(U_{n+h,m}^*(\tau))^2$ . Furthermore, using  $c(\tau, \tau) = \sum_{j=1}^\infty \lambda_j v_j^2(\tau)$ , where the convergence  $|c(\tau, \tau) - \sum_{j=1}^k \lambda_j v_j^2(\tau)| \rightarrow 0$ , as  $k \rightarrow \infty$ , is uniformly in

$\tau \in [0, 1]$ , see Theorem 7.3.5 of [Hsing & Eubank \(2015\)](#), we get that  $\sup_{\tau \in [0, 1]} E(U_{n+h, m}(\tau))^2 = \sup_{\tau \in [0, 1]} \sum_{j=m+1}^{\infty} \lambda_j v_j^2(\tau) \rightarrow 0$ . Therefore, and because  $E(X_{n+h, m}(\tau)U_{n+h, m}(\tau)) = 0$  for all  $\tau \in [0, 1]$ , to establish (29), it suffices by Cauchy-Schwarz inequality and the inequality  $\sup_{\tau \in [0, 1]} \sqrt{f(\tau)} \leq \sqrt{\sup_{\tau \in [0, 1]} f(\tau)}$ , where  $f$  is a non negative function on  $[0, 1]$ , to show that, in probability,

$$(I) \quad \sup_{\tau \in [0, 1]} |E(\sum_{j=1}^m \mathbf{1}_j^\top (\boldsymbol{\xi}_{n+h}^* \widehat{v}_j(\tau))^2 - E(\sum_{j=1}^m \mathbf{1}_j^\top \boldsymbol{\xi}_{n+h} v_j(\tau))^2| \rightarrow 0, \text{ and}$$

$$(II) \quad \sup_{\tau \in [0, 1]} E^*(U_{n+h, m}^*(\tau))^2 \rightarrow 0.$$

Consider (I). We have

$$\begin{aligned} |E(\sum_{j=1}^m \mathbf{1}_j^\top (\boldsymbol{\xi}_{n+h}^* \widehat{v}_j(\tau))^2 - E(\sum_{j=1}^m \mathbf{1}_j^\top \boldsymbol{\xi}_{n+h} v_j(\tau))^2| &\leq | \sum_{j_1, j_2=1}^m \mathbf{1}_{j_1}^\top (\Gamma_m^*(0) - \Gamma_m(0)) \mathbf{1}_{j_2} v_{j_1}(\tau) v_{j_2}(\tau) | \\ &\quad + | \sum_{j_1, j_2=1}^m \mathbf{1}_{j_1}^\top \Gamma_m^*(0) \mathbf{1}_{j_2} (\widehat{v}_{j_1}(\tau) \widehat{v}_{j_2}(\tau) - v_{j_1}(\tau) v_{j_2}(\tau)) | \\ &\leq \|\Gamma_m^*(0) - \Gamma_m(0)\|_F (\sum_{j=1}^m |v_j(\tau)|) \\ &\quad + \|\Gamma_m(0)\|_F \sum_{j=1}^m |\widehat{v}_j(\tau) - v_j(\tau)| (\sum_{j=1}^m |v_j(\tau)| + \sum_{j=1}^m |\widehat{v}_j(\tau)|). \end{aligned}$$

To evaluate the above terms notice that  $\|\Gamma_m(0)\|_F = O(1)$  and that by Lemma 9.1,  $\|\Gamma_m^*(0)\|_F = O_P(1)$ , where both bounds are uniform in  $m$ . Furthermore, using  $c(\tau, \tau) = \sum_{j=1}^{\infty} \lambda_j v_j^2(\tau)$  we get by the continuity of the kernel  $c(\cdot, \cdot)$  on the compact support  $[0, 1] \times [0, 1]$ , the bound  $\sum_{j=1}^m \lambda_j v_j^2(\tau) \leq c(\tau, \tau) \Rightarrow \sup_{\tau \in [0, 1]} \sum_{j=1}^m v_j^2(\tau) \leq \lambda_m^{-1} C$ , where  $C := \sup_{\tau \in [0, 1]} c(\tau, \tau) < \infty$ . Moreover, arguing as in [Kokoszka & Reimherr \(2013a\)](#), we get that  $\{m^{-1} \sum_{j=1}^m (\sqrt{n}(\widehat{v}_j(\tau) - v_j(\tau)))^2, \tau \in [0, 1]\}$  converges weakly which can be sharpened to  $\sup_{\tau \in [0, 1]} m^{-1} \sum_{j=1}^m n(\widehat{v}_j(\tau) - v_j(\tau))^2 = O_P(1)$ . Hence

$$\sum_{j=1}^m |\widehat{v}_j(\tau)| \leq \sqrt{m} \sqrt{\sum_{j=1}^m v_j^2(\tau)} + \sqrt{m} \sqrt{\sum_{j=1}^m (\widehat{v}_j(\tau) - v_j(\tau))^2} = O\left(\sqrt{\frac{m}{\lambda_m}} + \frac{m}{\sqrt{n}}\right),$$

and

$$\sum_{j=1}^m |\widehat{v}_j(\tau) - v_j(\tau)| (\sum_{j=1}^m |v_j(\tau)| + \sum_{j=1}^m |\widehat{v}_j(\tau)|) = O_P\left(\frac{m^{3/2}}{n \lambda_m^{1/2}} + \frac{m^2}{n^{3/2}}\right).$$

Therefore,

$$\sup_{\tau \in [0, 1]} |E(\sum_{j=1}^m \mathbf{1}_j^\top (\boldsymbol{\xi}_{n+h}^* \widehat{v}_j(\tau))^2 - E(\sum_{j=1}^m \mathbf{1}_j^\top \boldsymbol{\xi}_{n+h} v_j(\tau))^2| = O_P\left(\sqrt{\frac{m}{\lambda_m}} \|\Gamma_m^*(0) - \Gamma_m(0)\|_F\right) + o_P(1),$$

which vanishes because of Lemma 9.1 and Assumption 2'.

Consider (II). Since  $E^*(U_{n+h,m}^*(\tau))^2 \leq 2n^{-1} \sum_{t=1}^n (\widehat{U}_{t,n}^2(\tau))^2 + 2(\overline{U}_n(\tau))^2$ , it suffices to show that  $\sup_{\tau \in [0,1]} n^{-1} \sum_{t=1}^n (\widehat{U}_{t,n}(\tau))^2 \rightarrow 0$ . Toward this we use the bound

$$\begin{aligned} \frac{1}{n} \sum_{t=1}^n (\widehat{U}_{t,n}(\tau))^2 &\leq \frac{4}{n} \sum_{t=1}^n \|\widehat{\xi}_t - \xi_t\|_2^2 \sum_{j=1}^m v_j^2(\tau) + \frac{4}{n} \sum_{t=1}^n \|\widehat{\xi}_t\|_2^2 \sum_{j=1}^m (\widehat{v}_j(\tau) - v_j(\tau))^2 \\ &\quad + \frac{2}{n} \sum_{t=1}^n \left( \sum_{j=m+1}^{\infty} \xi_{j,t} v_j(\tau) \right)^2. \end{aligned} \quad (30)$$

Since

$$\sup_{\tau \in [0,1]} \frac{1}{n} \sum_{t=1}^n \|\widehat{\xi}_t - \xi_t\|_2^2 \sum_{j=1}^m v_j^2(\tau) \leq C \frac{1}{\lambda_m} \frac{1}{n} \sum_{t=1}^n \|\widehat{\xi}_t - \xi_t\|_2^2 = \frac{1}{\lambda_m} O_P\left(\frac{1}{n} \sum_{j=1}^m \frac{1}{\alpha_j^2}\right)$$

and

$$\sup_{\tau \in [0,1]} \frac{1}{n} \sum_{t=1}^n \|\widehat{\xi}_t\|_2^2 \sum_{j=1}^m (\widehat{v}_j(\tau) - v_j(\tau))^2 \leq O_P\left(\frac{m}{n}\right) \frac{1}{n} \sum_{t=1}^n \|\widehat{\xi}_t\|_2^2 = O_P\left(\frac{m}{n}\right),$$

the first two terms on the right hand side of (30) converge to zero. For the third term we get after evaluating the squared term and substituting  $\xi_{j,t} = \langle \mathcal{X}_t, v_j \rangle$  the bound,

$$\begin{aligned} \frac{1}{n} \sum_{t=1}^n (\mathcal{X}_t(\tau) - \sum_{j=1}^m \xi_{j,t} v_j(\tau))^2 &\leq \left| \frac{1}{n} \sum_{t=1}^n \mathcal{X}_t^2(\tau) - E\mathcal{X}_t^2(\tau) \right| \\ &\quad + \left| \sum_{j_1=1}^m \sum_{j_2=1}^m \langle (\widehat{\mathcal{C}}_0 - \mathcal{C}_0)(v_{j_1}), v_{j_2} \rangle v_{j_1}(\tau) v_{j_2}(\tau) \right| \\ &\quad + 2 \left| \sum_{j=1}^m \int_0^1 (\widehat{c}(\tau, s) - c(\tau, s)) v_j(s) ds v_j(\tau) \right| + \left| E\mathcal{X}_t^2(\tau) - \sum_{j=1}^m \lambda_j v_j^2(\tau) \right|. \end{aligned} \quad (31)$$

Now,  $\sup_{\tau \in [0,1]} |n^{-1} \sum_{t=1}^n (\mathcal{X}_t^2(\tau) - E\mathcal{X}_t^2(\tau))| = o_P(1)$  and for the last term of (31) we have,  $\sup_{\tau \in [0,1]} |E\mathcal{X}_t^2(\tau) - \sum_{j=1}^m \lambda_j v_j^2(\tau)| \rightarrow 0$ , by Theorem 7.3.5 of [Hsing & Eubank \(2015\)](#). Also

$$\begin{aligned} \sup_{\tau \in [0,1]} \left| \sum_{j_1=1}^m \sum_{j_2=1}^m \langle (\widehat{\mathcal{C}}_0 - \mathcal{C}_0)(v_{j_1}), v_{j_2} \rangle v_{j_1}(\tau) v_{j_2}(\tau) \right| &\leq \|\widehat{\mathcal{C}}_0 - \mathcal{C}_0\|_{HS} \sup_{\tau \in [0,1]} \left( \sum_{j=1}^m |v_j(\tau)| \right)^2 \\ &\leq m \|\widehat{\mathcal{C}}_0 - \mathcal{C}_0\|_{HS} \sup_{\tau \in [0,1]} \sum_{j=1}^m v_j^2(\tau) \\ &\leq C \frac{m}{\lambda_m} \|\widehat{\mathcal{C}}_0 - \mathcal{C}_0\|_{HS} = O_P\left(\frac{m}{\sqrt{n} \lambda_m}\right), \end{aligned}$$

which converges to zero. Finally, using

$$\begin{aligned} \left| \sum_{j=1}^m \int_0^1 (\widehat{c}(\tau, s) - c(\tau, s)) v_j(s) ds v_j(\tau) \right|^2 &\leq \int_0^1 (\widehat{c}(\tau, s) - c(\tau, s))^2 ds \left( \sum_{j=1}^m |v_j(\tau)| \right)^2 \\ &\leq \int_0^1 (\widehat{c}(\tau, s) - c(\tau, s))^2 ds m \sum_{j=1}^m v_j^2(\tau), \end{aligned}$$

we get

$$\begin{aligned} \sup_{\tau \in [0,1]} \left| \sum_{j=1}^m \int_0^1 (\widehat{c}(\tau, s) - c(\tau, s)) v_j(s) ds v_j(\tau) \right| &\leq C \sqrt{\frac{m}{\lambda_m}} \sqrt{\sup_{\tau \in [0,1]} \int_0^1 (\widehat{c}(\tau, s) - c(\tau, s))^2 ds} \\ &= O_P\left(\sqrt{\frac{m}{\lambda_m n}}\right) \rightarrow 0. \end{aligned}$$

□

**Proof of Corollary 3.1:** We elaborate only on the case  $h = 1$ . We have to show that  $\mathcal{E}_{n+1}^*$  converges weakly to  $\mathcal{E}_{n+1}$  in the space of continuous functions on the interval  $[0, 1]$ , equipped with the supremum norm  $\|\cdot\|_\infty$ , i.e.,  $(C([0, 1], \|\cdot\|_\infty))$ . We assume that the random element  $X_t(\tau), \tau \in [0, 1]$ , satisfies the required equicontinuity conditions and that the operator  $g$  is smooth with respect to  $\tau \in [0, 1]$  so that for all  $x \in \mathcal{H}$  and all  $\epsilon > 0$ , there exists  $\delta > 0$  such that  $\sup_{|\tau_1 - \tau_2| \leq \delta} |g(x)(\tau_1) - g(x)(\tau_2)| < \epsilon$ . The weak convergence of the finite dimensional distributions  $(\mathcal{E}_{n+1}^*(\tau_j), j = 1, 2, \dots, K)$  to  $(\mathcal{E}_{n+1}(\tau_j), j = 1, 2, \dots, K)$ , for every positive integer  $K$ , already has been established. It remains to show that for all  $\eta > 0$  and all  $\epsilon > 0$ , there exists  $\delta > 0$ , such that

$$\limsup_{n \rightarrow \infty} P^*\left(\sup_{|\tau_1 - \tau_2| < \delta} |\mathcal{E}_{n+1}^*(\tau_1) - \mathcal{E}_{n+1}^*(\tau_2)| > \epsilon\right) < \eta,$$

which by Markov's inequality is established if we show that  $\limsup_{n \rightarrow \infty} \epsilon^{-1} E^*\left(\sup_{|\tau_1 - \tau_2| < \delta} |\mathcal{E}_{n+1}^*(\tau_1) - \mathcal{E}_{n+1}^*(\tau_2)|\right) < \eta$ , in probability. Toward this goal, use the decomposition,

$$\begin{aligned} \mathcal{E}_{n+1}^*(\tau_1) - \mathcal{E}_{n+1}^*(\tau_2) &= \sum_{j=1}^m \xi_{j,t}^* (\widehat{v}_j(\tau_1) - \widehat{v}_j(\tau_2)) + (U_{n+1}^*(\tau_1) - U_{n+1}^*(\tau_2)) \\ &\quad + (\widehat{g}^*(X_n, \dots, X_{n-k+1})(\tau_1) - \widehat{g}^*(X_n, \dots, X_{n-k+1})(\tau_2)). \end{aligned}$$

To bound the first term use

$$\begin{aligned} E^*\left(\sup_{|\tau_1 - \tau_2| < \delta} \sum_{j=1}^m \xi_{j,t}^* (\widehat{v}_j(\tau_1) - \widehat{v}_j(\tau_2))\right) &\leq 2 \sum_{j=1}^m \sup_{\tau \in [0,1]} |\widehat{v}_j(\tau) - v_j(\tau)| (E^*(\xi_{j,t}^*)^2)^{1/2} \\ &\quad + \sum_{j=1}^m \sup_{|\tau_1 - \tau_2| < \delta} |v_j(\tau_1) - v_j(\tau_2)| (E^*(\xi_{j,t}^*)^2)^{1/2}, \end{aligned}$$

which can be made arbitrarily small using the arguments of the proof of Theorem 3.2 and the equicontinuity properties of the  $v_j$ 's. Bounding the second term of the decomposition used, it turns out that the corresponding bound is dominated by the term  $n^{-1} \sum_{t=1}^n \sup_{|\tau_1 - \tau_2| < \delta} |U_t(\tau_1) - U_t(\tau_2)|$  which can be made arbitrarily small using the stochastic equicontinuity of the random element  $U_t(\tau) = X_t(\tau) - \sum_{j=1}^m \xi_{j,t} v_j(\tau), \tau \in [0, 1]$ . Finally using the notation  $\mathbf{X}_{n,k} = (X_n, X_{n-1}, \dots, X_{n-k+1})$ ,

the last term is bounded by

$$E^* \left( \sup_{|\tau_1 - \tau_2| < \delta} |\widehat{g}^*(\mathbf{X}_{n,k})(\tau_1) - \widehat{g}^*(\mathbf{X}_{n,k})(\tau_2)| \right) \leq 2 \sup_{\tau \in [0,1]} E^* |\widehat{g}^*(\mathbf{X}_{n,k})(\tau) - g(\mathbf{X}_{n,k})(\tau)| \\ + \sup_{|\tau_1 - \tau_2| < \delta} |g(\mathbf{X}_{n,k})(\tau_1) - g(\mathbf{X}_{n,k})(\tau_2)|.$$

## References

- Ahn, S. C. & Horenstein, A. R. (2013), ‘Eigenvalue ratio test for the number of factors’, *Econometrica* **81**(3), 1203–1227.
- Alonso, A. M., na, D. P. & Romo, J. (2002), ‘Forecasting time series with sieve bootstrap’, *Journal of Statistical Planning and Inference* **100**(1), 1–11.
- Antoniadis, A., Brossat, X., Cugliari, J. & Poggi, J.-M. (2016), ‘A prediction interval for a function-valued forecast model: Application to load forecasting’, *International Journal of Forecasting* **32**, 939–947.
- Antoniadis, A., Paparoditis, E. & Sapatinas, T. (2006), ‘A functional wavelet-kernel approach for time series prediction’, *Journal of the Royal Statistical Society: Series B* **68**(5), 837–857.
- Aue, A., Norinho, D. D. & Hörmann, S. (2015), ‘On the prediction of stationary functional time series’, *Journal of the American Statistical Association: Theory and Methods* **110**(509), 378–392.
- Berlinet, A., Elamine, A. & Mas, A. (2011), ‘Local linear regression for functional data’, *Annals of the Institute of Statistical Mathematics* **63**(5), 1047–1075.
- Billingsley, P. (1999), *Converges of Probability Measures*, John Wiley & Sons, New York.
- Boj, E., Delicado, P. & Fortiana, J. (2010), ‘Distance-based local linear regression for functional predictors’, *Computational Statistics & Data Analysis* **54**(2), 429–437.
- Bosq, D. (2000), *Linear processes in function spaces*, Lecture notes in Statistics, New York.
- Bosq, D. & Blanke, D. (2007), *Inference and Prediction in Large Dimensions*, John Wiley & Sons, Chichester.
- Breidt, F. J., Davis, R. A. & Dunsmuir, W. T. M. (1995), ‘Improved bootstrap prediction intervals for autoregressions’, *Journal of Time Series Analysis* **16**(2), 177–200.

- Cheng, R. & Pourahmadi, M. (1993), ‘Baxter’s inequality and convergence of finite predictors of multivariate stochastic processes’, *Probability Theory and Related Fields* **95**, 115–124.
- Chiou, J.-M. & Müller, H.-G. (2009), ‘Modeling hazard rates as functional data for the analysis of cohort lifetables and mortality forecasting’, *Journal of the American Statistical Association: Applications and Case Studies* **104**(486), 572–585.
- Cuevas, A., Febrero, M. & Fraiman, R. (2006), ‘On the use of the bootstrap for estimating functions with functional data’, *Computational Statistics and Data Analysis* **51**(2), 1063–1074.
- Dehling, H., Sharipov, S. O. & Wendler, M. (2015), ‘Bootstrap for dependent Hilbert space-valued random variables with application to von Mises statistics’, *Journal of Multivariate Analysis* **133**, 200–215.
- Ferraty, F. & Vieu, P. (2006), *Nonparametric Functional Data Analysis*, Springer, New York.
- Ferraty, F. & Vieu, P. (2011), Kernel regression estimation for functional data, in F. Ferraty & Y. Romain, eds, ‘The Oxford Handbook of Functional Data Analysis’, Oxford University Press, Oxford.
- Findley, D. F. (1986), Bootstrap estimates of forecast mean square errors for autoregressive processes, in D. M. Allen, ed., ‘Computer Science and Statistics: the Interface’, Elsevier Science, pp. 11–17.
- Franke, J. & Nyarige, E. G. (2019), A residual-based bootstrap for functional autoregressions, Technical report, University of Kaiserslautern.  
**URL:** <https://arxiv.org/abs/1905.07635>
- Gneiting, T. & Raftery, A. E. (2007), ‘Strictly proper scoring rules, prediction and estimation’, *Journal of the American Statistical Association: Review Article* **102**(477), 359–378.
- Goldsmith, J., Greven, S. & Crainiceanu, C. (2013), ‘Corrected confidence bands for functional data using principal components’, *Biometrics* **69**(1), 41–51.
- Hörmann, S., Kidziński, L. & Hallin, M. (2015), ‘Dynamic functional principal components’, *Journal of the Royal Statistical Society: Series B* **77**(2), 319–348.
- Hörmann, S. & Kokoszka, P. (2010), ‘Weakly dependent functional data’, *Annals of Statistics* **38**(3), 1845–1884.

- Hörmann, S. & Kokoszka, P. (2012), Functional time series, *in* T. S. Rao, S. S. Rao & C. R. Rao, eds, ‘Handbook of Statistics’, Vol. 30, North Holland, Amsterdam, pp. 157–186.
- Horváth, L. & Kokoszka, P. (2012), *Inference for Functional Data with Applications*, Springer, New York.
- Horváth, L., Kokoszka, P. & Rice, G. (2014), ‘Testing stationarity of functional time series’, *Journal of Econometrics* **179**(1), 66–82.
- Hsing, T. & Eubank, R. (2015), *Theoretical Foundations of Functional Data Analysis, with An Introduction to Linear Operators*, John Wiley & Sons, New York.
- Hurvich, C. M. & Tsai, C.-L. (1993), ‘A corrected Akaike information criterion for vector autoregressive model selection’, *Journal of Time Series Analysis* **14**(3), 271–279.
- Hyndman, R. J. & Shang, H. L. (2009), ‘Forecasting functional time series (with discussions)’, *Journal of the Korean Statistical Society* **38**(3), 199–221.
- Kokoszka, P. & Reimherr, M. (2013a), ‘Asymptotic normality of the principal components of functional time series’, *Stochastic Processes and Their Applications* **123**(5), 1546–1562.
- Kokoszka, P. & Reimherr, M. (2013b), ‘Determining the order of the functional autoregressive model’, *Journal of Time Series Analysis* **34**(1), 116–129.
- Kokoszka, P., Rice, G. & Shang, H. L. (2017), ‘Inference for the autocovariance of a functional time series under conditional heteroscedasticity’, *Journal of Multivariate Analysis* **162**, 32–50.
- Kudraszow, N. L. & Vieu, P. (2013), ‘Uniform consistency of  $k$ NN regressors for functional variables’, *Statistics and Probability Letters* **83**(8), 1863–1870.
- Masry, E. (2005), ‘Nonparametric regression estimation for dependent functional data: asymptotic normality’, *Stochastic Processes and their Applications* **115**(1), 155–177.
- McMurry, T. & Politis, D. N. (2011), Resampling methods for functional data, *in* F. Ferraty & Y. Romain, eds, ‘The Oxford Handbook of Functional Data Analysis’, Oxford University Press, New York, pp. 189–209.
- Meyer, M. & Kreiss, J.-P. (2015), ‘On the vector autoregressive sieve bootstrap’, *Journal of Time Series Analysis* **36**(3), 377–397.

- Pan, L. & Politis, D. N. (2016), ‘Bootstrap prediction intervals for linear, nonlinear and nonparametric autoregression’, *Journal of Statistical Planning and Inference* **177**, 1–27.
- Panaretos, V. M. & Tavakoli, S. (2013), ‘Fourier analysis of stationary time series in function space’, *Annals of Statistics* **41**(2), 568–603.
- Paparoditis, E. (2018), ‘Sieve bootstrap for functional time series’, *Annals of Statistics* **46**(6B), 3510–3538.
- Paparoditis, E. & Sapatinas, T. (2016), ‘Bootstrap-based testing of equality of mean functions or equality of covariance operators for functional data’, *Biometrika* **103**(3), 727–733.
- Pascual, L., Romo, J. & Ruiz, E. (2004), ‘Bootstrap predictive inference of ARIMA processes’, *Journal of Time Series Analysis* **25**(4), 449–465.
- Pilavakis, D., Paparoditis, E. & Sapatinas, T. (2019), ‘Moving block and tapered block bootstrap for functional time series with an application to the  $K$ -sample mean problem’, *Bernoulli* **25**(4B), 3496–3526.
- Politis, D. N. & Romano, J. P. (1994), ‘The stationary bootstrap’, *Journal of the American Statistical Association: Theory and Methods* **89**(428), 1303–1313.
- Ra a, P., Aneiros, G., Vilar, J. & Vieu, P. (2016), ‘Bootstrap confidence intervals in functional nonparametric regression under dependence’, *Electronic Journal of Statistics* **10**(2), 1973–1999.
- Ra a, P., Aneiros-Perez, G. & Vilar, J. M. (2015), ‘Detection of outliers in functional time series’, *Environmetrics* **26**(3), 178–191.
- Shang, H. L. (2015), ‘Resampling techniques for estimating the distribution of descriptive statistics of functional data’, *Communications in Statistics-Simulation and Computation* **44**(3), 614–635.
- Shang, H. L. (2017), ‘Functional time series forecasting with dynamic updating: An application to intraday particulate matter concentration’, *Econometrics and Statistics* **1**, 184–200.
- Shang, H. L. (2018), ‘Bootstrap methods for stationary functional time series’, *Statistics and Computing* **28**(1), 1–10.
- Thombs, L. A. & Schucany, W. R. (1990), ‘Bootstrap prediction intervals for autoregression’, *Journal of the American Statistical Association: Theory and Methods* **85**(410), 486–492.

- Vilar, J., Aneiros, G. & Raña, P. (2018), ‘Prediction intervals for electricity demand and price using functional data’, *International Journal of Electrical Power and Energy Systems* **96**, 457–472.
- Yao, F., Müller, H. & Wang, J. (2005), ‘Functional data analysis for sparse longitudinal data’, *Journal of the American Statistical Association: Theory and Methods* **100**(470), 577–590.
- Zhu, T. & Politis, D. N. (2017), ‘Kernel estimates of nonparametric functional autoregression models and their bootstrap approximation’, *Electronic Journal of Statistics* **11**(2), 2876–2906.